약학석사 학위논문

붉은 대극에서 분리, 정제한 Ebractenoid F의 항염 활성 기전에 대한 연구

Anti-inflammatory Mechanism of a Diterpenoid, Ebractenoid F, Isolated from *Euphorbia ebracteolata* Hayata

2018 년 2 월

서울대학교 대학원

약학과 천연물과학 전공

마 상 연

ABSTRACT

Anti-inflammatory Mechanism of a Diterpenoid, Ebractenoid F, Isolated from *Euphorbia ebracteolata* Hayata

Sang Yeon Mah

Natural Products Science

College of Pharmacy

Master Course in the Graduate School

Seoul National University

Euphorbia ebracteolata Hayata, belongs to Euphorbiaceae, is widely distributed through the south of China. In the traditional chinese medicine (TCM), the roots of *E. ebracteolata* have been prescribed for chronic inflammation-mediated diseases such as tracheitis, cutaneous tuberculosis, tumor, and psoriasis. It has been reported that *E. ebracteolata* is rich in bioactive components such as acetophenones, flavonoids, and diterpenes. Among the constituents of *E. ebracteolata*, diterpenes

in *E. ebracteolata* have effects on anti-inflammation, anti-tumor, and anti-fungal activities. However, the anti-inflammatory mechanism of most of constituents in *E. ebracteolata* Radix is not yet fully discovered.

For find the anti-inflammatory compound from *E. ebracteolata* Radix, bioassay-guided fractionation, which is a general way to isolate and characterize bioactive compounds from natural products, was conducted. It might be a worth way to find out the most potential compounds possessing biological activities. Thus, we applied this concept to process separation. In addition, a separation method, called high speed counter-current chromatography (HSCCC), was co-operated because it provides us many advantages in terms of high yield, sample loading capacity, easy scale-up, purity, and resolution. Following the bioassay-guided isolation, the compounds were elucidated and identified by various spectroscopic ways. Ebractenoid F (EF) showing the potential effects was ultimately obtained by this method, bioassay-guided isolation.

Inflammation is a key factor of protection system triggered by immune cells in response to harmful stimuli. It mediates various cellular processes such as proliferation, cell cycle, and differentiation. If the stimuli remain, the acute inflammatory response is connected to the chronic inflammatory response. The nitric oxide (NO) and SEAP are the inflammatory mediators, so they could arise from the inflammation. In this vein of thought, we seek for anti-inflammatory agents which can reverse both NO and SEAP production regulated by NF-κB.

EF shows the prominent inhibition of NF-κB Secretary Alkaline Phosphatase (SEAP) (IC_{50} = 7.71 μM), implying that it is specifically targeting on NF-κB. It

decreases the downstream of NF-κB including various pro-inflammatory mediators, such as inducible nitric oxide synthase (iNOS), cyclooxygenase-2 (COX-2), and interleukin-6 (IL-6), at both protein and mRNA levels. Moreover, it down-regulates phosphorylation and degradation of inhibitory κB (IκB)-α in 20 minutes. Nuclear translocation and transcriptional activity are suppressed when cells are treated with EF. In addition, we investigated whether it has an effect on LPS-induced mitogen-activated protein kinase (MAPKs, p-ERK, and p-JNK) and the upstream signaling pathways (p-AKT and p-IKK).

Taken together, we tried to find the anti-inflammatory compound from *E. ebracteolata* using bioassay-guided fractionation in that there are not enough studies. At this research, we could discover a potential compound, ebractenoid F (EF). Through this achievement, we also expected that inflammation-mediated diseases can be managed with this compound since the NF-κB signaling pathway related to inflammation was suppressed. Although we still need to study on the effect of ebractenoid F, it is possible to be a key regulator on inflammation-related to diseases.

Keyworkds: *Euphorbia ebracteolata* Hayata, HSCCC, NF-κB, RAW 264.7 cell

Student Number: 2016-21847

CONTENTS

LIST OF FIGURES

LIST OF TABLES

LIST OF ABBREVIATIONS

ATCC	American Type Culture Collection
COSY	Correlation Spectroscopy
DMEM	Dulbecco's Modified Eagle's Medium
d	Doublet
D-PBS	Distortionless Enhancement by Polarization Transfer
DMSO	Dimethyl Sufoxide
EtOH	Ethyl Alcohol
ELSD	Evaporative Light Scattering Detector
EF	Ebractenoid F
FBS	Fetal Bovine Serum
HEPES	N-2-Hydroxyethylpiperazine-N-2-Ethane Sulfonic Acid
HPLC	High Performance Liquid Chromatography
HSCCC	High Speed Counter Current Chromatography
HSQC	Heteronuclear Single Quantum Coherence
HMBC	Heteronuclear Multiple Bond Coherence

MeOH	Methyl Alcohol
MTT	2-(4,5-dimethylthiazol-2-yl)-2,5-diphenyltetrazoliumbromide
NMR	Nuclear Magnetic Resonance
PCR	Polymerase Chain Reaction
s	Singlet
t	Triplet
ROESY	Rotating-frame nuclear Over Hauser Enhancement Spectroscopy

Ⅰ. INTRODUCTION

1. Bioassay-guided Isolation

Bioassay-guided fractionation is one of the fundamental separation procedures using various analytical methods along with defined biological activities [1]. Generally, bioactive compounds from natural products can be isolated and the natural products can be characterized by this method [2-3]. The common separation scheme is in Figure 1. Also, it might be a worth way to find out the most promising compounds possessing biological activities because it is an effective way to cut off the time for isolating potential compounds [3]. The method starts with examining the extract of natural products. After confirmed the activities, the further fractionation is performed. The active fraction is selected using bioassays, and the selected fraction is further separated. The inactive fractions are stored or discarded. All process is repeated at every single step isolating the active fractions until single bioactive compounds are obtained. Then, the isolated pure compounds are determined or identified by diverse spectroscopic methods [2-3].

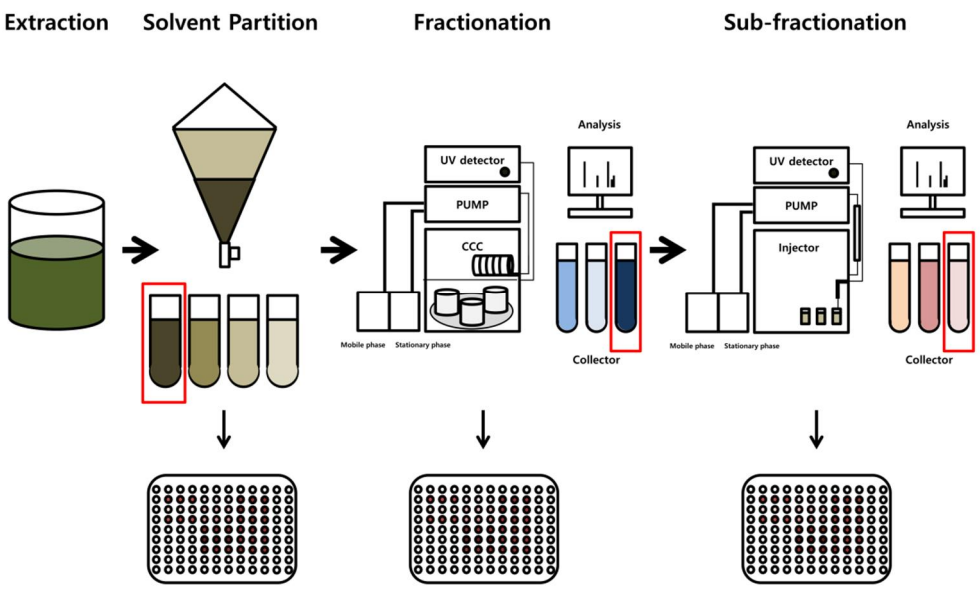

Figure 1. General scheme of bioassay guided fractionation

The plant materials are extracted and sequentially partitioned with solvents. After confirmed their bioactivities with specific bioassays, the most potent one is being subject to further separation using various analytical machines. Biological activities are measured at every single stage; a certain fraction is selected to be isolated according to the results. The process is being repeated until the pure compounds are obtained. And then the compounds are elucidated and determined by spectroscopic methods.

2. Inflammation

Inflammation is a critical factor of defense system triggered by immune cells in response to harmful stimuli such as microbial pathogens, chemicals, and irritants. This response also facilitates the repair, turnover, and adaptation of many tissues. Acute inflammation rapidly occurs in which several key mediators are released to the infection region under tissue injury or invading pathogen [4]. If the stimuli persist, or defense signaling is not working, acute inflammation can progress to chronic inflammation that can initiate disease development [5-11]; atherosclerosis, psoriasis, Alzheimer's disease (AD), type 2 diabetes mellitus, rheumatoid arthritis, and even cancer. (Figure 2)

Many inflammatory diseases are incurable, but steroid treatments and non-steroidal anti-inflammatory drugs (NSAIDs) are widely used for relieving inflammatory symptoms like redness, pain, heat, and swelling. However, long-term steroid and NSAIDs treatment evokes side-effects [4].

Induction of inflammation by microbial components is dependent on activation of resident immune cells present in macrophages, mast cells and dendritic cells. These immune cells have pattern recognition receptors (PRRs) like pathogen-associated molecular patterns (PAMPs) and damage-associated molecular patterns (DAMPs). PAMPs are associated with various pathogens, whereas DAMPs are with host-related injury and cell damage [12]. Between them, Toll-like receptors (TLRs) signaling pathway by PAMPs is generally used as an inflammatory *in vitro* model system; lipopolysaccharides (LPS)-induced RAW 264.7 macrophages. TLRs are shown to relate to inflammatory genes. TLR4 is an essential receptor against LPS,

and can be activated by LPS. Macrophage activation mediated by LPS arises from inflammation. And, the release of inflammatory mediators is necessary for the progression of chronic inflammatory-related numerous diseases through the downstream signaling of TLR4 [13].

TLR4 pathway has two ways (Figure 3); MyD88-dependent and independent signaling pathways. MyD88-dependent pathway recruits interleukin (IL)-1 receptor-associated kinase (IRAK) 1/4, TNF receptor-associated factor 6 (TRAF 6) activating transforming growth factor-β-activated kinase 1 (TAK1), sequentially IκB kinase (IKK) and mitogen-activated protein kinase (MAPK) pathways. MyD88-independent pathway activates Toll IL-1 receptor domain-containing adaptor-inducing IFN- β (TRIF), co-stimulating several molecules (CD40, CD80, and CD86) and affecting on the transcription factor IRF3, NF-κB, and MAPK. The former one is responsible for pro-inflammatory cytokine expression, whereas the latter one is for the induction of Type Ⅰ interferons and interferon-inducible genes [13-14].

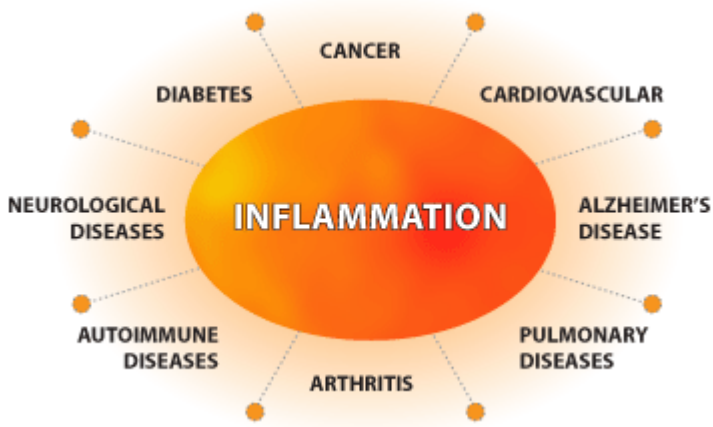

Figure 2. Inflammation regulating several diseases

Several diseases are linked with acute and chronic inflammation.

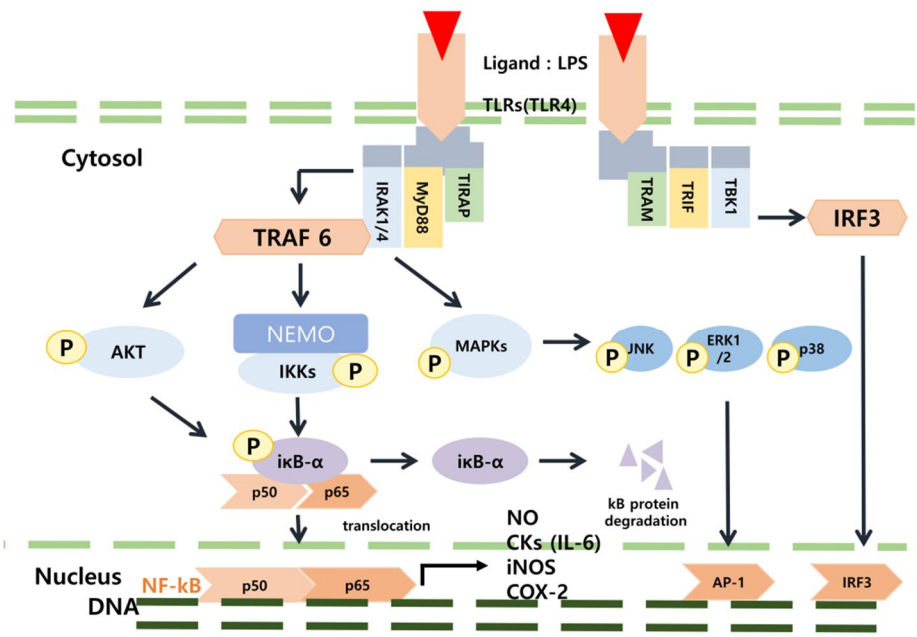

Figure 3. Signaling pathway of toll-like receptor 4 (TLR4)

3. *Euphorbia ebracteolata* Hayata

Euphorbia ebracteolata Hayata belongs to Euphorbiaceae family. It distributes in the south of China, Jiangsu, Anhui, Zhejiang, and Fujian. Over the south of China, it also grows in Asia including Japan and Korea. *E. ebracteolata* has been widely used with other plants which are *Euphorbia fischeriana* and *Stellera chamaejasme* as "Lang Du". Lang Du comprising *E. ebracteolata* is well known as a traditional medicine for treating several chronic inflammation, including tracheitis, tuberculosis, and psoriasis [15, 16]. In addition, it is reported that *E. ebracteolata* contains acetophenones, flavonoids, and diterpenoids [17-25]. Especially, diterpenoids are isolated from the medicinal herb show anti-inflammation, anti-tumor, and anti-fungal activities [19-21]. The roots have been reported to possess various anti-inflammatory compounds [21]. Since there is little known about its anti-inflammatory mechanism study in detail, it is worth focusing on *E. ebracteolata*.

Figure 4. Shoots and roots of *E. ebracteolata*

4. Nuclear Factor-κB (NF-κB)

NF-κB is a pivotal transcription factors mediating the cellular processes such as cellular interaction, recruitment, and signaling communication. The family of NF-κB includes NF-κB1 (p50/p105), NF-κB2 (p52/p100), RelA (p65), RelB, and c-Rel and shares a Rel homology domain in their N-terminus. The C-terminus regions of RelA, RelB, and c-Rel have NF-κB transactivation domain [26].

In an inactive state, nuclear factor of kappa light polypeptide gene enhancer in B-cells inhibitors are composed of IκB-α/β/ε, and inhibit nuclear localization signals of NF-κB proteins and keep them sequestered in an inactive state in the cytosol [27]. A wide range of signals, which are typically cytokines, environmental particles, toxic metals, intracellular stresses, viral or bacterial products, and UV light, can activate NF-κB mediated by Toll signaling pathway related to inflammatory genes expression [28]. In an active state, IκB kinase (IKK) consisting of IKK-α/β subunits phosphorylates two serine residues, followed by a modification process called ubiquitination [29]. It leads to degradation of IκB by proteasome and simultaneous translocation of NF-κB dimer from cytosol to nucleus. Activated NF-κB binds to κB-sites in nucleus, regulates transcription mediating inflammatory activities [27-29].

When NF-κB is transcribed, inflammatory mediators such as nitric oxide (NO), secretary alkaline phosphatase (SEAP), and various cytokines, are secreted. Among them, NO assay is one of the accepted methods for screening inflammatory agents since high NO levels are generated in response to inflammatory stimuli and involved in the occurrence of inflammation [30]. It is a crucial role in host immune

defense, vascular regulation, neuronal signal transduction, and other systems [31]. In addition, NF-κB SEAP can be the selective way to discover the candidate fractions/compounds when the target mechanism is related to NF-κB. Once NF-κB is activated in the cells harboring NF-κB plasmid, it secretes SEAP [32]. In this vein of thought, measuring NO and SEAP production from the supernatants are typical methods to discover anti-inflammatory agents [30-32].

To sum up, these successive pathways (TLR4-mediated NF-κB-inflammatory mediators) can orchestrate inflammation with other biological responses; proliferation, differentiation, and pro- or anti-apoptotic reactions. The prolonged NF-κB activation can induce various inflammation-related diseases.

5. High Speed Counter-Current Chromatography (HSCCC)

High speed counter-current chromatography (HSCCC) was devised as a kind of continuous liquid-liquid partition chromatography [33, 34]. The method offers advantages over the conventional separation way [33-37]. The advantage of HSCCC is that separation can be operated without solid stationary phase. Therefore, there is no irreversible adsorption of sample onto the solid phase as common in conventional chromatography [33]. In addition, a large amount of sample can be injected, leading to obtain a large amount of fractions as well as constituents with high purity in a single separation [35]. The scale-up from milligrams to grams in drug discovery is significant, and is easily possible with HSCCC [35]. In addition, it is used for enhancing the performance and increasing the selectivity of liquid chromatography [36]. Like above mentioned, it provides us many advantages in terms of high yield, sample loading capacity, easy scale-up, purity, and resolution. Because of these advantages, many researches have tried to co-operate the HSCCC in separation [35-37].

HSCCC is mainly driven by the planetary motion (Figure 5) [38]. The holder surrounding multilayer coils is rotating its own axis and revolves at the centrifuge frame. It is designed that the coils are not twisted under the planetary motion. The motion provides two major functions for performing CCC separation: a rotary-seal-free elution so that the mobile phase is continuously eluted through the rotating isolation column; a unique hydrodynamic motion of two solvent phases in the rotating multilayer coiled column. The coils are filled with liquid-liquid solvent system in an end-closed coiled system. When the rotation starts, the solvent system

injected to HSCCC is divided into the lighter and heavier phase at each end of the coiled column. The solute (target compound) in the column is subjected to the repetitive partition process of mixing and settling at an enormously high rate of over 13 times per second (at 800 rpm).

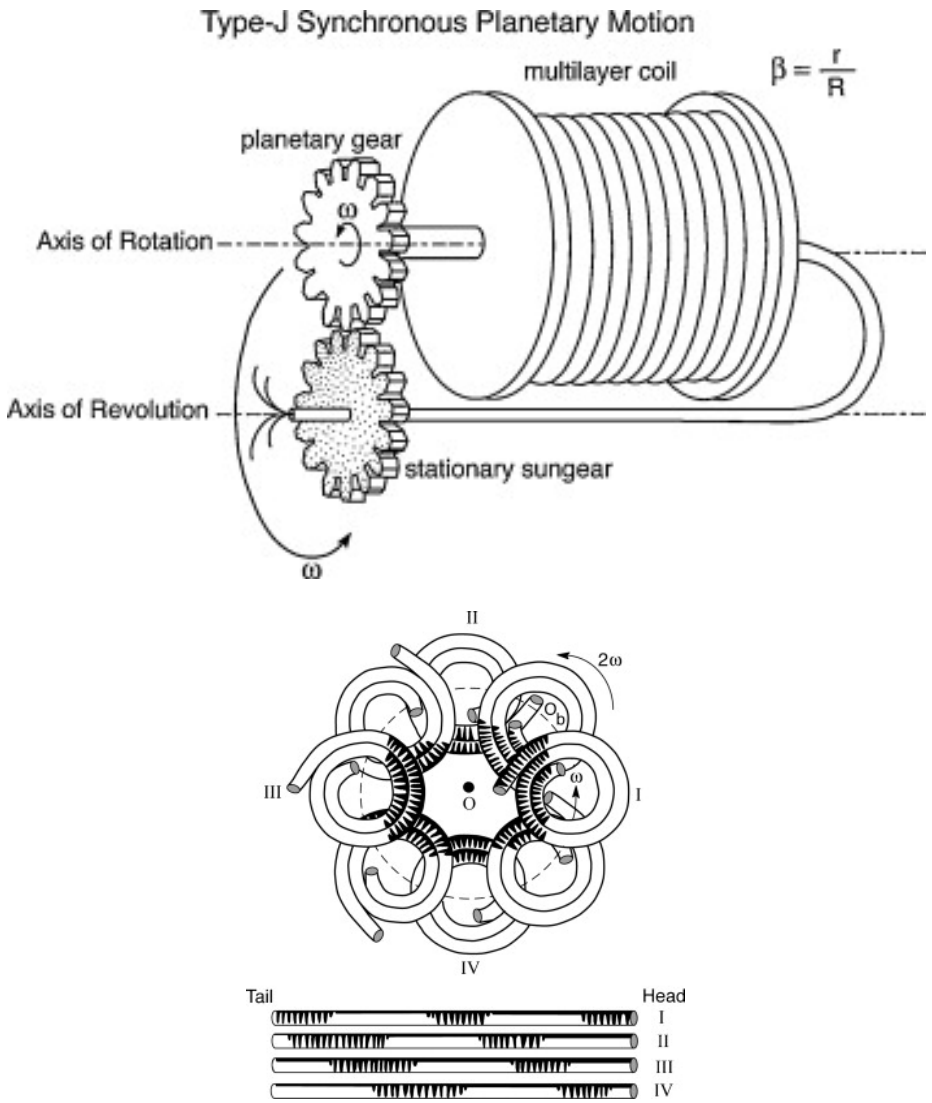

Figure 5. The principle of HSCCC

6. Purpose of This Study

The root of *E. ebracteolata* are used with other two medicinal herbs (*Euphorbia fischeriana* and *Stellera chamaejasme*) for treating several chronic inflammation, including tracheitis, tuberculosis, and psoriasis. Among three plants, two of them (*E. ebracteolata* and *E. fischeriana*) have their appearance, ethno pharmaceutical uses, and even constituents in common [15]. However, they are definitely different herbs each other [16]. In our study, since *E. fischeriana* has been studied intensively, *E. ebracteolata* is chosen to investigate chemistry and biology.

Some researchers have reported that *E. ebracteolata* contains acetophenone, flavonoids, and diterpenes. Especially, diterpenes have shown the promising biological activities, such as anti-inflammation, anti-tumor, and anti-fungal activity. Although a lot of compounds isolated from this herb are known for anti-inflammatory effects [20, 21], the anti-inflammatory mechanism is not fully understood. Thus, the purposes of this study are to discover the most potent anti-inflammatory compound, to investigate the pharmaceutical mechanism for the first time, and to identify the bioactive compound via bioassay-guided fractionation.

Ⅱ. MATERIALS & METHODS

1. MATERIALS

1.1 Plant materials

The dried roots of *Euphorbia ebracteolata* Hayata were purchased from Korea Traditional Medicinal plant market (Kyung-dong market, Seoul, Republic of Korea). The specimen purchased from Kyung-dong market was identified as *Euphorbia ebracteolata* H. by Professor Young Bae Suh at the College of Pharmacy, Seoul National University (Seoul, Republic of Korea).

1.2 Chemicals and reagents

Most of organic solvents used for extraction, column chromatograph, and HSCCC, such as formic Acid (FA), acetonitrile (ACN), *n*-hexane (*n*-Hex), methylene chloride (MC), ethylene acetate (EA), *n*-butanol (*n*-BuOH), distilled water (DW) and methanol (MeOH), were purchased from Dae Jung Science (Seoul, Korea). The HPLC-grade acetonitrile was supplied by J.T. Baker (Phillipsburg, NJ). Distilled water (NANO pure Diamond, Barnstead, USA) was used for all solutions and dilutions. DMSO (purity: >99.9%) dissolving certain substrates for the cell culture were purchased from Sigma-Aldrich Co. (St. Louis, MO). DMSO (purity: >99%) for MTT assay was obtained from Duksan Co.

For the cell culture, Dulbecco's Modified Eagles' Medium (DMEM), fetal bovine

serum (FBS), penicillin and streptomycin, HEPES buffer solution, and G418 were purchased from GenDepot (Baker, TX). Dulbecco's Phosphate Buffered Saline (DPBS), *Escherichia coli* LPS, 5-diphenyltetrazolium bromide (MTT), and protease inhibitor cocktail were obtained from Sigma-Aldrich Co. (St. Louis, MO). The antibodies for iNOS, COX-2, p-IκBα, IκBα, p50, p65, p-AKT, AKT, p-IKKα/β, IKKα/β, MyD88, TIRAP, p-JNK, JNK, p-ERK, ERK, p-p38, p38, and β-actin were purchased from Santa Cruz Biotechnology (Santa Cruz, CA). All other chemicals and reagents were purchased from Sigma-Aldrich Co. unless otherwise indicated.

1.3 Instruments

HPLC analyses were carried out on Hitachi L-6200 instrument equipped with Hitachi L-4000 UV detector and SIL-9A auto injector (Shimadzu, Japan). INNO C_{18} column (I.D. 4.6 mm x 150 mm, 5 μm particle size) was purchased from Young Jin biochrom Co. Ltd (Seongnam, South Korea).

Preparative HPLC separation was performed using Hitachi JP/L-7100 equipped with Hitachi L-4000 UV detector. INNO C_{18} column (I.D. 100 mm x 250 mm, 10 μm particle size) was purchased from Young Jin biochrom Co. Ltd (Seongnam, South Korea).

The CCC instrument used in the present study was a TBE-1000A (Tauto Biotech., Shanghai, China), including a six-port injection valve, a 60 mL sample loop, a Hitachi L-6200 pump and a Hitachi UV detector L-7400 (Hitachi, Tokyo, Japan). The TBE01000A had three multilayer coil separation columns connected in series

(tube I.D. 3.0 mm, each volume of three coils: 330 mL, total volume: 1000 mL). The rotation speed of the apparatus ranged from 0 to 500 rpm.

The mass spectrometry analyses were performed using a Finniga LCQ ion trap mass spectrometer from Thermo Finnigan (San Jose, CA) equipped with an electrospray (ESI) probe.

The NMR analyses were recorded on Bruker Avance 500 spectrometers. ^{1}H and ^{13}C NMR spectra were measured in a $CDCl_3$ solution at 500 and 125 MHz, respectively.

The molecular biological machines were illustrated in each method section.

2. METHODS

2.1 Solvent extraction of *Euphorbia ebracteolata* Hayata

The dried and chopped roots of *E. ebracteolata* (5 kg) were extracted with methanol (5 x 18 L) by ultra-sonication at room temperature for 12h. After filtration, the extract was evaporated under reduced pressure, and the dried extract (125.9 g, 4.196% yield) was suspended in distilled water, and sequentially partitioned with *n*-Hex (3 x 2.5 L), MC (3 x 2.5 L), EA (3 x 2.5 L), *n*-BuOH (3 x 2.5 L), and DW (3 x 2.5 L). The evaporated extract and fractions were stored in a refrigerator (4℃) for the subsequent HSCCC separation.

2.2 Sub-fractionation of *Euphorbia ebracteolata* Hayata using High Speed Counter Current Chromatography (HSCCC)

The *n*-Hex fraction (39.2 g) was dissolved in *n*-Hex:80% acetonitrile (1:1, v/v). The lower phase was filtered and dried using a rotary vacuum evaporator. The dried fraction was suspended in EtOH and then subjected to HSCCC filled with *n*-Hex as the upper phase (the stationary phase). And, the lower phase (the mobile phase) was pumped into the system at a flow rate of 3 mL/min while the columns were rotating at a speed of 460 rpm. The HSCCC solvent condition for *n*-Hex fraction was as follows: eluent A: DW with 0.1 % FA; B: ACN with 0.1% FA; gradient: 0-200 min (40-80% B), 200-250 min (80-100% B) and then washed with 100% B until 400 min. The UV system detection was performed at 280 nm and 2.5 absorbance units. The sub-fractions were collected according to the elution profile

and analyzed by HPLC-UV. Twelve sub-fractions (H1-H12) were obtained from the *n*-Hex fraction using HSCCC. The dried sub-fractions were stored in a refrigerator (4℃) for the further separation.

2.3 Isolation of an anti-inflammatory compound via preparative-HPLC

The H10 sub-fraction (502 mg) was dissolved in MeOH and injected into the preparative-HPLC to give 6 fractions (H10-1~H10-6). The prep-HPLC conditions for H10 sub-fraction was as follows: A: DW with 0.1 % FA; B: ACN with 0.1% FA; gradient: 0-15 min (45-65% B); 15-40 min (65-100% B) and then washed with 100% B for 9 min at a flow rate of 3 mL/min, UV detection at 280 nm. The final fractions (H10-1-H10-6) were collected according to each peak on the HPLC-UV chromatogram and were stored in a refrigerator (4℃) for the further experiments.

2.4 HPLC analysis

An INNO C_{18} column (4.6 mm x 150 mm, 5 μm particle size) was used to analyze the extract, fractions (solvent partition), sub-fractions (HSCCC), and three compounds at the last separation step. The injection volume was 20 μL. For analysis of each separation step, the mobile phase was optimized with water with 0.1 % FA (A) and ACN with 0.1 % FA (B). The gradient system was following: 0-15 min (45-65% B); 15-40 min (65-100% B) and then equilibrated with 100% B for 9 min at a flow rate of 0.8 mL/min. The column was at room temperature and the UV detection was conducted at 280 nm.

2.5 Identification of isolated compounds

Isolated compounds were analyzed with HPLC-MS coupled with electrospray ionization source (ESI-MS) for molecular weight and the visible wavelength. Also, the structure of compounds dissolved in $CDCl_3$ was identified by comparing the ^{1}H and ^{13}C NMR spectra in $CDCl_3$ with references, and two-dimensional (2D) NMR spectra (Bruker Avance 500-MHz, National Center for Interuniversity Research Facilities at Seoul National University).

2.6 Cell culture

The RAW 264.7 cell, which was derived from murine macrophages, was obtained from the American Type Culture Collection (Manassas, VA). These cells were maintained in DMEM medium, supplemented with 10% FBS, 100 U/mL penicillin, and 100 μg/mL streptomycin at 37℃ in a 5% CO_2 incubator. The RAW 264.7 cells harboring a p-NF-κB secretory alkaline phosphatase (SEAP)-NPT reporter construct were cultured under the same conditions, except that the culture medium was supplemented with 500 μg/mL geneticin (G418, GenDepot).

2.7 Cellular viability assay

The cell viability was measured by a 3-(4,5-dimethylthiazol-2-yl)-2,5-diphenyltetrazolium bromide (MTT) assay. The cells were seeded into 24-well plates at a density of 10^5 cells per well and maintained at 37℃ in a humidified 5% CO_2 incubator for 24 h. The cells were pretreated with ebractenoid F or TPCK as the positive control for 2 h followed by LPS (1 μg/mL) treatment. After 18-24 h incubation, the MTT solution (0.5 mg/mL) was added to each well, and then incubated for 2 h. Following removal of media, the formazan crystals were dissolved in 500 μL of DMSO. One hundred micro-liters of the dissolved solution were transferred to 96-well plates and the absorbance was detected at 595 nm wavelength using an Emax microplate reader (Molecular Devices; Sunnyvale, CA). The relative cell viability was calculated and compared with the absorbance of the untreated control group. All experiments were performed in triplicate.

2.8 The measurement of Nitric oxide (NO) production

The RAW 264.7 cells were seeded into 24-well plates at 10^5 cells per well. After 24 h incubation, the cells were treated with the indicated concentration of EF and TPCK as a positive control for 2 h, followed by LPS (1 μg/mL) treatment for 18 h. One hundred micro-liters of supernatant were transferred to 96-well plates, and then was mixed with 100 μL of Griess reagent (1% sulfanilamide in 5% phosphoric acid and 0.1% naphtylethylenediamine dihydrochloride in distilled water). The optical density was measured at 540 nm. The nitric oxide production was calculated from a standard curve of sodium nitrite solutions.

2.9 NF-κB SEAP reporter gene assay

The pNF-κB-SEAP-NPT plasmid activates the secretary alkaline phosphatase (SEAP) reporter gene in response to NF-κB activation and also encodes the neomycin phosphotransferase (NPT) gene for geneticin resistance in host cells. This plasmid was constructed and transfected into RAW 264.7 cells. The transfected RAW 264.7 cells were pretreated with ebractenoid F for 2 h prior to LPS (1 μg/mL) treatment. After 16 h LPS stimulation, the fluorescence from the product of the SEAP/MUP reaction was measured in relative fluorescence units (RFU) by a 96-well plate fluorimeter (Gemini XS, Molecular Devices, Sunnyvale, CA) at an excitation of 360 nm and an emission of 449 nm.

2.10 NF-κB luciferase assay

For investigation NF-κB promoter activity, plasmid DNA was prepared by Fast DNA-spin ^{TM} Plasmid DNA Purification Kit (iNtRON Biotechnology, Seongnam, Korea). RAW 264.7 cells were transiently transfected with the prepared pCMV-Luc and pNF-κB-Luc reporter vector using transfection reagent (Intron Biotechnology, Seoul, Korea) according to the manufacturer's instructions. After 24 h incubation, cells were untreated or pretreated for 2 h with ebractenoid F, followed by LPS (1 μg/mL) stimulation for 6-8 h in 24-well plates. Each well was then washed with PBS and cells were lysed by 1X passive lysis buffer diluted in PBS. Luciferase activity of the target gene was determined using a Dual-Luciferase Reporter Assay System (Promega, Madison, WI, USA) according to the manufacturer's instructions. The luminescence signal was measured using a luminometer (MicroLumat Plus, Berthold Technologies, Dortmund, Germany).

2.11 Western blot analysis

RAW 264.7 cells were treated with Ebractenoid F for 2 h, followed by LPS (1 μg/mL) treatment for the indicated time. After incubation, whole cell lysates were lysed with lysis buffer [20 mM HEPES (pH 7.6), 350 mM NaCl, 20% glycerol, 0.5 mM EDTA, 0.1mM EGTA, 1% Nonidet P-40 (NP-40), 50 mM NaF, 0.1mM dithiothreitol (DTT), 0.1 mM phenylmethylsulfonyl fluoride (PMSF) and protease inhibitor cocktail]. Cytoplasmic and nuclear fractions were prepared using the previously described lysis buffer. The proteins were quantified using the Bradford

protein assay (Bio-Rad Laboratories, Richmond, CA). Equal amounts of protein (15-25 μg) were loaded on 7-10% SDS polyacrylamide gels and transferred to nitrocellulose membranes using a wet transfer system (Bio-Rad, Hercules, CA). The membranes were blocked by 5% BSA in T-BST buffer (20 mM Tris, 137 mM NaCl, 0.1% Tween 20, pH 7.6) and incubated with primary antibodies (1:1000 dilution in T-BST buffer) overnight in 4℃. After washing, the membranes were incubated with horseradish peroxidase (HRP)-conjugated secondary antibodies (1:3000 dilution in T-BST buffer) for 1-2 h at room temperature. The immunoblots were visualized with WEST-ZOL® Plus luminol-based ECL reagent (iNtRON, Seongnam, Korea).

2.12 Quantitative real-time reverse transcriptase polymerase chain reaction (real-time PCR)

RAW 264.7 cells were pretreated with ebractenoid F for 2 h, and then LPS (1 μg/mL) for 18 h. After incubation, the total RNAs were extracted using the Trizol reagent kit (Invitrogen, Carlsbad, CA). Both the amount and purity of RNAs were measured using the Nanodrop spectrophotometer (Thermo Scientific, Wilmington, DE). The cDNA was synthesized from one microgram of total RNAs using the amfiRivert Platinum cDNA Synthesis Master Mix (GenDepot, Barker, TX) according to the manufacturer's instructions. Quantitative real-time reverse transcription polymerase chain reaction (RT-PCR) analysis for iNOS, COX-2, IL-6, IL-1β, MCP-1 and β-actin was performed with an Applied Biosystems 7300 real-time PCR system and the software (Applied Biosystems, Carlsbad, CA).

Quantitative real-time PCR was performed using forward and reverse primers and a SYBR Green working solution (AccuPower® 2XGreenStar qPCR Master Mix, Bioneer, Daejeon, Korea), with the following conditions: 95℃ for 30 s, followed by 40 cycles of 95℃ for 15 s, 55℃ for 20 s, and 72℃ for 35 s. The following primers were used (Table 1): iNOS, 5'-TCC TAC ACC ACA CCA AAC-3' (sense) and 5'-CTC CAA TCT CTG CCT ATC C-3' (antisense); COX-2, 5'-CCT CTG CGA TGC TCT TCC-3' (sense) and 5'-TCA CAC TTA TAC TGG TCA AAT CC-3' (antisense); IL-6, 5'-AGG CTT AAT TAC ACA TGT TCT CTG G-3' (sense) and 5'-TTA TAT CCA GTT TGG TAG CAT CCA T-3' (antisense); IL-1β, 5'-GCC ACC TTT TGA CAG TGA TGA G-3' (sense) and 5'-AGT GAT ACT GCC TGC CTG AAG-3' (antisense); MCP-1, 5'-ATG CAG TTA ATG CCC CAC TC-3' (sense) and 5'-TTC CTT ATT GGG GTC AGC AC-3' (antisense); GAPDH, 5'-GCC ATC AAT GAC CCC TTC ATT-3' (sense) and 5'-GCT CCT GGA AGA TGG TGA TGG-3' (antisense); β-actin, 5'-CTG ACT ACC TCA TGA AGA TCC TC-3' (sense) and 5'-CAT TGC CAA TGG TGA TGA CCT G-3' (antisense).

Table 1. Primer sequences of inflammatory medicators

Gene	5'-Forward primer-3'	5'-Reverse primer-3'
iNOS	TCCTACACCACACCAAAC	CTCCAATCTCTGCCTATCC
COX-2	CCTCTGCGATGCTCTTCC	TCACACTTATACTGGTCAAATCC
MCP-1	ATGCAGTTAATGCCCCACTC	TTCCTTATTGGGGTCAGCAC
IL-6	AGGCTTAATTACACATGTTCTCTGG	TTATATCCAGTTTGGTAGCATCCAT
IL-1β	GCCACCTTTTGACAGTGATGAG	AGTGATACTGCCTGCCTGAAG
β-actin	CTGACTACCTCATGAAGATCCTC	CATTGCCAATGGTGATGACCTG
GAPDH	GCCATCAATGACCCCTTCATT	GCTCCTGGAAGATGGTGATGG

2.13 Preparation of the cytoplasmic and nuclear extract

RAW 264.7 cells were treated with ebractenoid F for 2 h prior to LPS (1 μg /mL) stimulation. The cells were washed and suspended in 100 μL of iced-cold lysis buffer A [10 mM HEPES [pH 7.9], 10 mM KCl, 0.2 mM EDTA, 0.1 mM EGTA, 1 mM DTT, 1 mM PMSF and a protease inhibitor cocktail] for cytoplasmic extract on ice for 15 min. After ice incubation, 12.5 μL of 10% NP-40 was added. The tubes were agitated on a vortex for 20 s and then centrifuged for 5 min. The resulting supernatant represented the cytosolic extract. The remain pellets were the nuclear extract. The pellets were resuspended in 20 μL of ice-cold nuclear extraction buffer (20 mM HEPES [pH 7.9], 400 mM NaCl, 1 mM EDTA, 1 mM EGTA, 1 mM DTT, 0.4mM PMSF and a protease inhibitor cocktail) and incubated on ice for 1 h with intermittent vortexing. This nuclear extract was centrifuged for 10 min at 15,000 rpm; the resulting supernatant represented the nuclear fraction.

2.14 *Statistical analysis*

The results represent the mean ± the standard deviation (SD) from three different experiments. A one-way analysis of variance (ANOVA) followed by a Dunnett's *t*-test was applied to assess the statistical significance of the differences between the study groups. P values < 0.05 were considered statistically significant [$*P < 0.05$; $**P < 0.01$; $***P < 0.001$].

Ⅲ. RESULTS

1.Isolation of Ebractenoid F (EF) from *E. ebracteolata* by bioassay-guided fractionation

The bioassay-guided fractionation was performed to isolate the most effective bioactive compound. The subject fractions for isolation were selected by bioassays at every single step (Figure 6). Five kilograms of *Euphorbia ebracteolata* Hayata was grinded and extracted with 18 L of methanol for 6 h at the room temperature. This process was repeated for five times. After filtration, the extracts were evaporated under reduced pressure and lyophilized. The methanol extract (125.9 g) was partitioned with *n*-hexane (*n*-Hex), methylene chloride (MC), ethyl acetate (EA), *n*-butanol (*n*-BuOH), and distilled water (DW) at 1:1 ratio for three times (Figure 7). All fractions were evaporated to be dried under vacuum. The *n*-Hex fraction (39.2 g), which potentially reduced nitric oxide (NO) production at the non-toxic dose on the RAW 264.7 cells, was selected to be sub-fractionated and thoroughly evaporated. Thirty grams of *n*-Hex fraction was dissolved in 80% acetonitrile and sub-fractionated using high speed counter current chromatography (HSCCC, Tauto TBE-1000A, Shanghai Tauto Biotech Co. Ltd, Shanghai, China) (Figure 8). The H10 sub-fraction (502 mg) was finally isolated by preparative-HPLC to obtain pure compounds. Among the compounds, H10-6 (77 mg) was selected because it showed the most valuable anti-inflammatory effects (Figure 9).

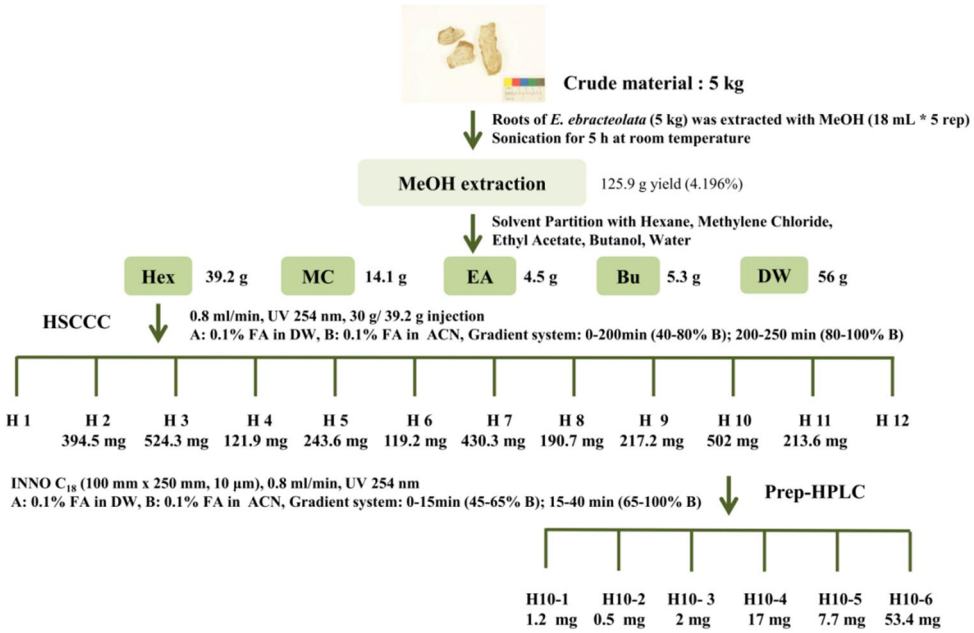

Figure 6. Separation scheme of *E. ebracteolata*

E. ebracteolata was extracted with MeOH, and sequentially partitioned with *n*-Hex, MC, EA, *n*-BuOH, and DW. The *n*-Hex layer (30 g of 39.2 g) was injected into HSCCC to obtain 12 sub fractions. After then, the selected H10 sub fraction was further isolated using preparative HPLC.

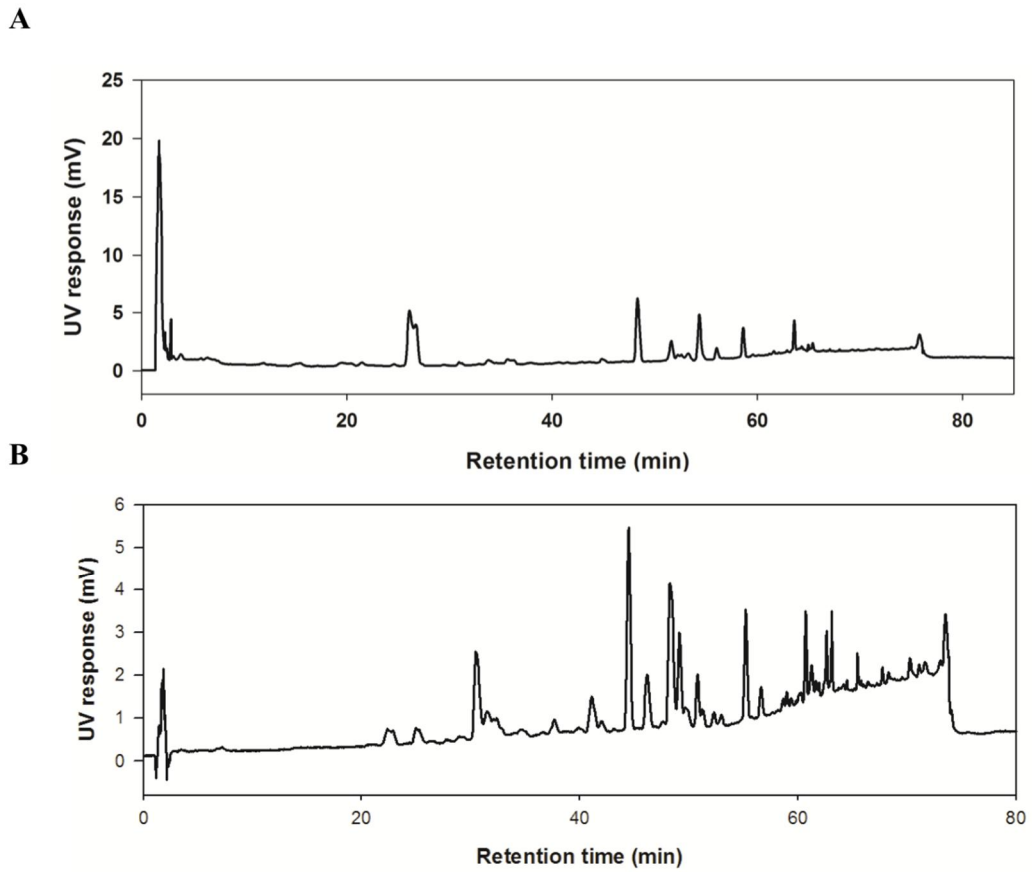

Figure 7. HPLC-UV chromatogram of (A) MeOH extract and (B) *n*-Hex fraction

(A) The total MeOH extract of *E. ebracteolata* (B) The *n*-Hex fraction which includes less polar components in *E. ebracteolata*. The mobile phases were composed of 0.1% formic acid in water and 0.1% formic acid in acetonitrile. The flow rate of 0.8 mL/min was employed with INNO C_{18} column (I.D. 4.6 mm x 150 mm, 5 μm particle size) in HPLC-UV analysis. The gradient system was illustrated in section 2.1.

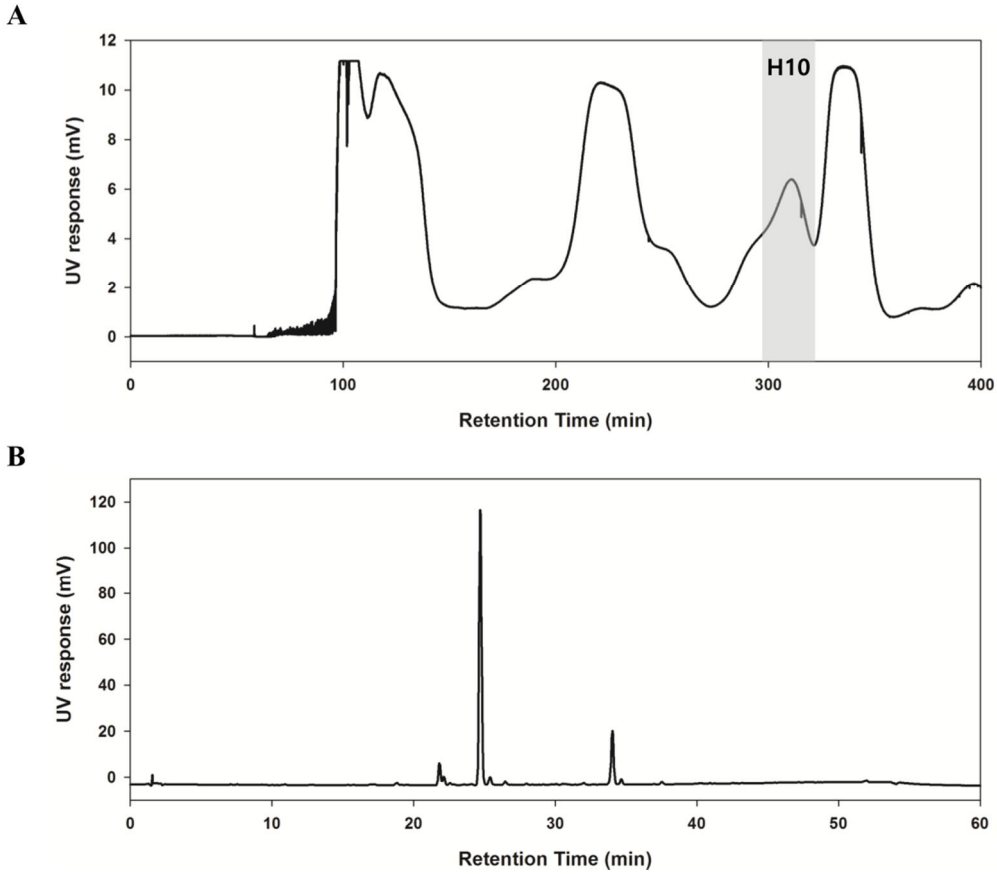

Figure 8. (A) HSCCC chromatogram of *n*-Hex fraction and (B) HPLC-UV chromatogram of H10 sub-fraction

(A) The HSCCC chromatogram of *n*-Hex layer. The grey region, designated as H10, was collected from 290 to 320 min. H10 was selected as the most potential fraction in the *n*-Hex layer. (B) The HPLC-UV chromatogram of H10 sub-fractionated from the *n*-Hex layer. Following solvent partition at the previous experiment, *n*-Hex was subjected to be separated by HSCCC. The 0.1% formic acid in *n*-Hex was used as the stationary phase, 0.1% formic acid in acetonitrile, and 0.1% formic acid in distilled water were used as the mobile phase. The flow rate of 3 mL/min and revolution speed of 460 rpm were employed in HSCCC separation. The gradient system was illustrated in section 2.2.

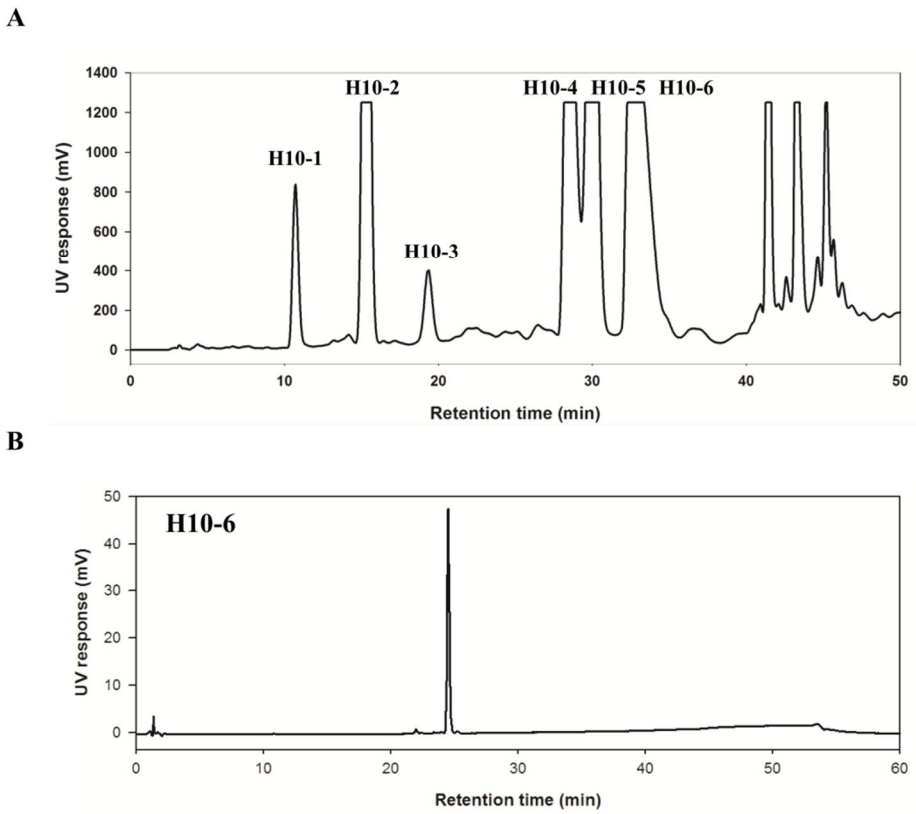

Figure 9. (A) Preparative-HPLC chromatogram of H10 sub-fraction and (B) HPLC-UV chromatograms of separated compounds

(A) The prep-HPLC chromatogram of H10 sub-fraction. (B) The HPLC-UV chromatograms of pure compounds, H10-4, H10-5, and H10-6, isolated from the sub-fractionated H10 layer. Following the previous sub-fractionation using HSCCC, H10 was subjected to be purified by preparative-HPLC. The mobile phases were composed of 0.1% formic acid in water and 0.1% formic acid in acetonitrile. The flow rate of 3 mL/min was employed with INNO C_{18} column (100 mm x 250 mm, 10 μm particle size) in prep-HPLC. The gradient system was illustrated in section 2.3.

2.Screening fractions/compounds from *E. ebracteolata*

To access the anti-inflammatory potency of extracts, fractions, sub-fractions, and compounds from *E. ebracteolata*, anti-inflammatory effects were evaluated at the nontoxic doses. First of all, we determined the cytotoxicity of them on RAW264.7 cells using MTT assay. And then, nitric oxide (NO) and NF-κB Secretary Alkaline Phosphatase (SEAP) assay were applied at each separation step. The results were shown in Table 2.

First, the roots of *E. ebracteolata* were extracted with methanol, and the extract showed promising reduction of nitric oxide (NO) at the nontoxic dose (IC_{50} = 1.1 ± 0.2 μg/ml). Next, the methanol extract was partitioned with solvents (*n*-Hex, MC, EA, *n*-BuOH, and DW). Among the solvent fractions, the solvent fraction which exhibited the most effective NO reduction was the *n*- Hex fraction (IC_{50} = 2.4 ± 0.2 μg/mL). For the further separation, the *n*- Hex fraction was sub-fractioned using HSCCC to offer 12 sub-fractions. All the sub-fractions had outstanding NO suppression. Hence, NF-κB Secretary Alkaline Phosphatase (SEAP) assay was used to screen samples in that NO production could be evoked by the NF-κB signaling pathway. Based on the results of NF-κB SEAP inhibitory effects, the H10 sub-fraction exhibited the most promising anti-inflammatory effect (IC_{50} = 4.0 ± 1.7 μg/mL). Finally, the H10 sub-fraction was separated into the final fractions (H10-1~H10-6) using preparative-HPLC. Among them, the three compounds, including H10-4, H10-5, and H10-6, were elucidated as pure compounds. As shown in Figure 10, H10-6 was chosen to explore its bioactive mechanism for the further study (IC_{50} = 7.7 ± 0.82 μM).

Extr/ Frc	[a]IC_{80} (μg/ml)	[b]IC_{50} (μg/ml)	[c]IC_{50} (μg/ml)
MeOH ext	-	1.11 ± 0.26	N.D.
n-Hex	-	2.39 ± 0.23	N.D.
MC	-	6.00 ± 0.27	N.D.
EA	-	>20	N.D.
n-Bu	-	> 20	N.D.
DW	-	> 20	N.D.
H1	>20	<1	>20
H2	>20	<1	-
H3	>20	<1	>20
H4	8.82	<1	3.06 ± 1.28
H5	3.01	<1	8.74 ± 2.06
H6	>20	<1	>20
H7	>20	<1	7.51 ± 0.89
H8	>20	<1	>20
H9	2.38	<1	5.96 ± 0.86
H10	11.91	<1	4.01 ± 1.68
H11	1.36	<1	8.81 ± 1.85
H12	>20	<1	-
H10-1	>20	12.46 ± 0.07	>20
H10-2	>20	3.33 ± 0.05	>20
H10-3	>20	4.82 ± 1.24	>20
H10-4	>20	<0.83	1.76 ± 1.2
H10-5	19.92	5.95 ± 2.24	>7.8
H10-6	19.53	<0.715	2.21 ± 0.82

Table 2. Inhibitory effects of extract, fractions, sub-fractions, and compounds on LPS-induced NO and NF-κB SEAP production in macrophage RAW 264.7 cells

Cells (1 X 10^5 cells/well) were seeded in 24-well plates and incubated for 24 h. After then, cells were pretreated with the different doses of all the samples

including MeOH extract, solvent partitions, CCC fractions, prep-HPLC sub-fractions, and single compounds for 2 h before LPS (1 μg/mL) stimulation. Cell viability was determined by MTT assay after 24 h sample treatment. NO production was estimated by NO assay after 18h LPS stimulation, and NF-κB SEAP was measured after 16 h LPS treatment.

[a]: IC_{80} by MTT assay; [b]: IC_{50} by NO assay; [c]: IC_{50} by SEAP assay; IC_{50}: half maximal inhibitory concentration; -: no effect; N.D.: not determined

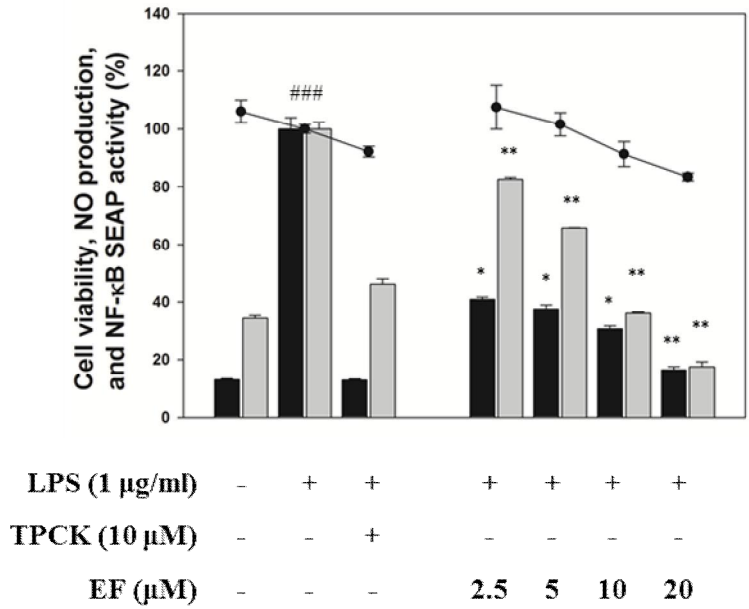

Figure 10. The effects of the selected H10-6 on LPS-stimulated inflammatory mediators, NO and NF-κB SEAP, in macrophages

Cells (1 X 10^5 cells/well) were seeded in 24-well plates and incubated for 24 h. After then, cells were pretreated with the indicated doses of the sample for 2 h before LPS (1 μg/mL) stimulation. Cell viability was determined by MTT assay after 24 h sample treatment. NO production was estimated by NO assay after 18 h LPS stimulation, and NF-κB SEAP was measured after 16 h LPS treatment. Data were obtained from three independent experiments and expressed as the mean ± standard deviation (S.D).

3.Elucidation and Determination of Ebractenoid F (EF)

The fraction H10-6 was analyzed and the purity was accessed by HPLC-UV and HPLC-MS. In addition, the chemical structure of the isolated compound was determined based on the 1D/2D NMR data.

H10-6 is obtained as yellow oil. Its molecular formula is determined to be $C_{19}H_{24}O_2$ based on ESI-MS at *m/z* 287 $[M+H]^+$ and NMR analysis ($CDCl_3$). It is detected under UV (MeOH) $\lambda_{max}(\log\varepsilon)$ 220/280 nm. The ^1H and ^{13}C NMR data of H10-6 indicated that it is an 18-norrosane diterpenoid with an aromatic A-ring. According to the ^1H NMR ($CDCl_3$, 500 MHz), one proton (H-15) at δ 5.86 (dd, *J*= 17.4, 10.8 Hz) and two protons (H-16 and H-16') at δ 4.87 (dd, *J*= 10.8, 0.9 Hz) and 4.95 (dd, 17.4, 0.9 Hz) indicate the terminal methylene group. The HMBC correlations from H-1 to C-3 (δ 139.9), C5 (δ 127.1), and C9 (36.4), from H-6 to C-4 (δ 122.6), C-5 (δ 127.1), and C-10 (δ 140.4), from Me-19 to C-3 (δ 139.9), C-4 (δ 122.6), and C-5 (δ 127.1), and from 3-OH to C-2 (δ 140.8), C-3 (δ 139.9), and C-4 (δ 122.6), reveal the presence of a 3,4,5-trisubstituted catechol as ring A. The relative configuration is determined by the ROESY spectrum. The correlations of Me-20/H-12β, H-12β/H-15, and H-8/Me-17 indicate a β-orientation for Me-20 and α-orientations for H-8 and Me-17 (Figure 12-17, and Table 3). Thus, the chemical structure of H10-6 was defined as shown in figure 11 and represents ebractenoid F (EF).

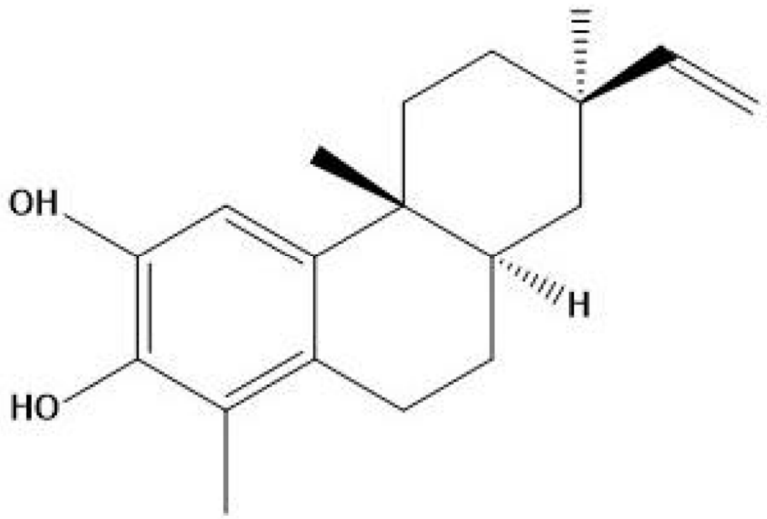

Figure 11. Chemical structure of ebractenoid F

The isolated compound was determinated by 1D/2D NMR and MS spectrometry. H10-6 was called Ebractenoid F (EF).

A

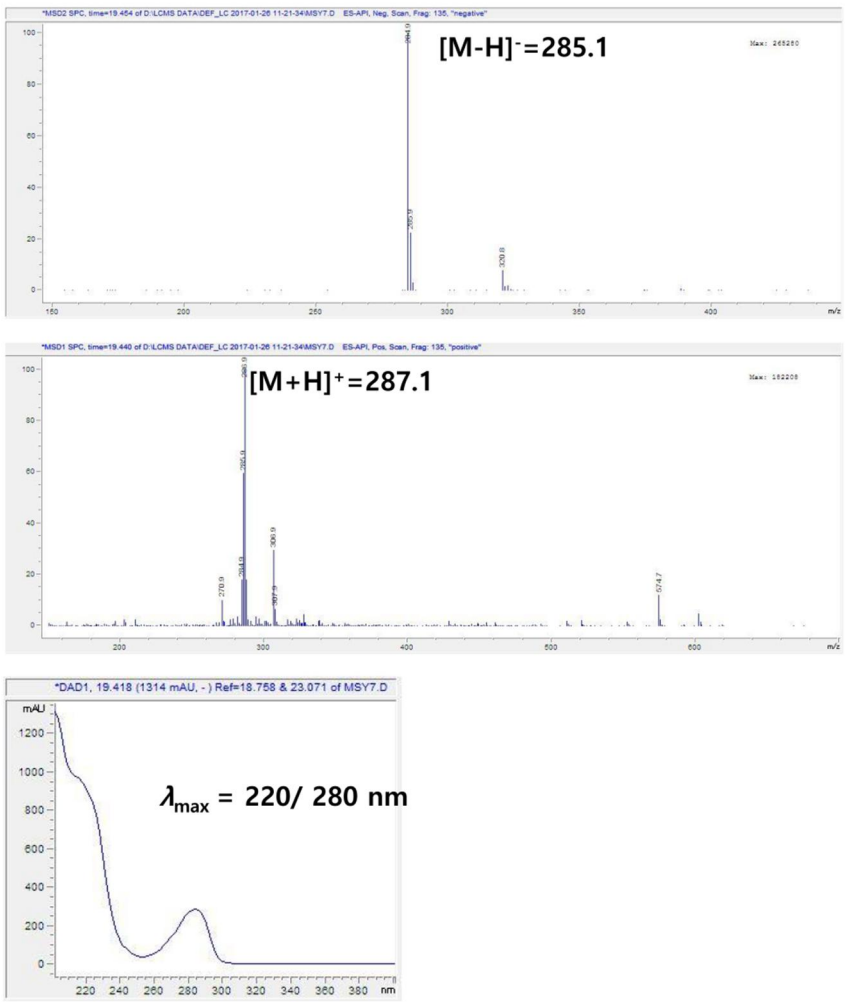

Figure 12. LC-ESI/MS spectra and UV spectrum of H10-6 (EF)

The H10-6 (EF) generated the protonated ions $[M+H]^+$ at *m/z* 287.1 in positive ion mode and the deprotonated ions $[M-H]^-$ at *m/z* 285.1 in negative ion mode. The compound has maximum UV absorption at 220 and 280 nm.

Table 3. ^{1}H and ^{13}C NMR assignment of H10-6 (EF) (δ in ppm, J in Hz, 500 and 125 MHz in $CDCl_3$)

position	δ_H (J in Hz)	δ_C
1	6.7, s	108.8
2		140.8
3		139.9
4		122.6
5		127.1
6	2.64, m	26.9
7	1.55, m 1.64, m	25.7
8	1.64, m	36.4
9		36.4
10		140.4
11	1.57, m 1.95, m	34.1
12	1.37, m 1.66, m	32.9
13		36.4
14	1.19, m 1.44, m	39.6
15	5.86, dd (17.4, 10.8)	151.1
16	4.88, dd (10.8, 0.9) 4.96, dd (17.4, 0.9)	108.9
17	1.02, s	22.8
18		
19	2.11, s	11.4
20	1.01, s	21.3

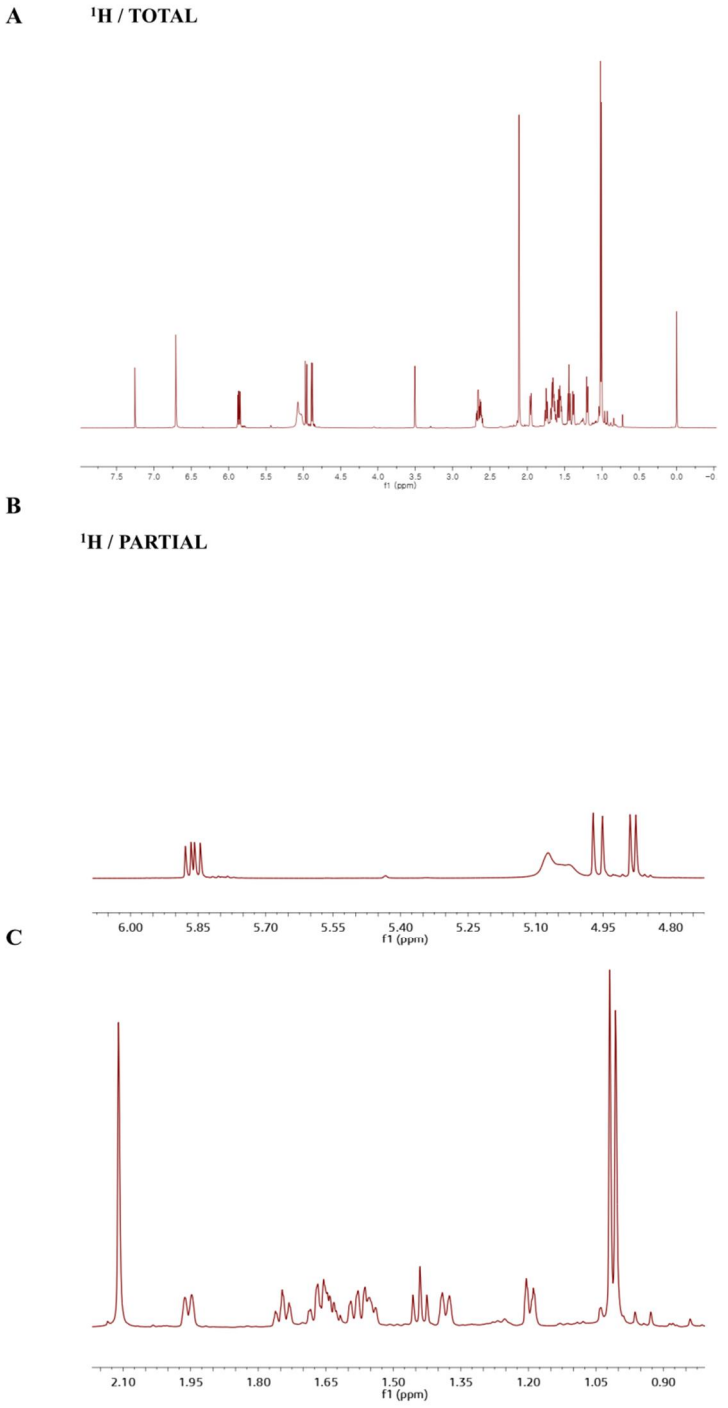

Figure 13. ^{1}H NMR spectra of H10-6 (EF) (Dissolved in $CDCl_3$, 500 MHz)

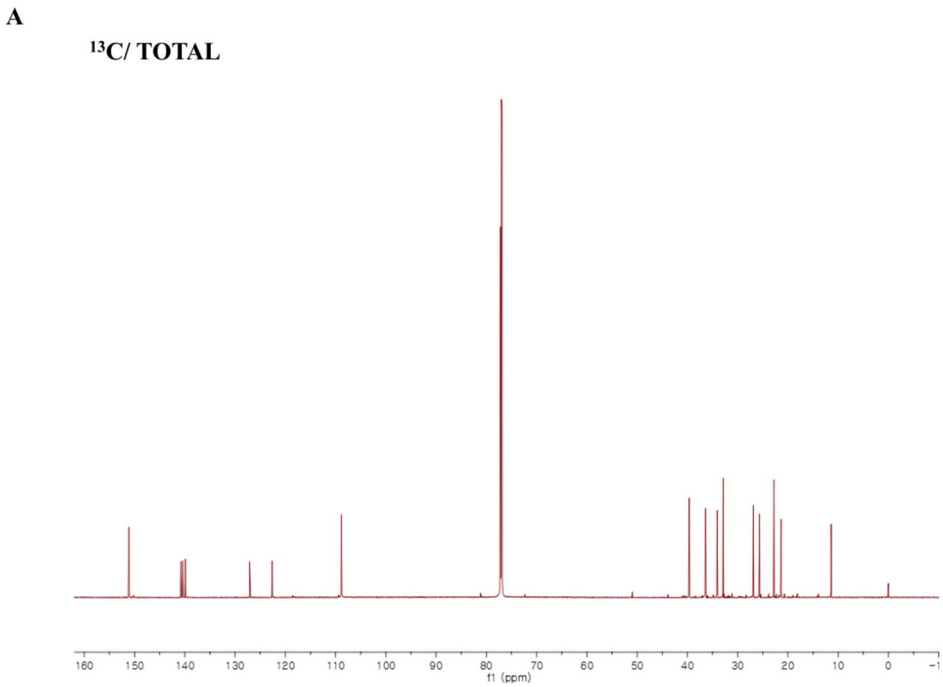

Figure 14. ^{13}C NMR spectra of H10-6 (EF) (Dissolved in $CDCl_3$, 125 MHz)

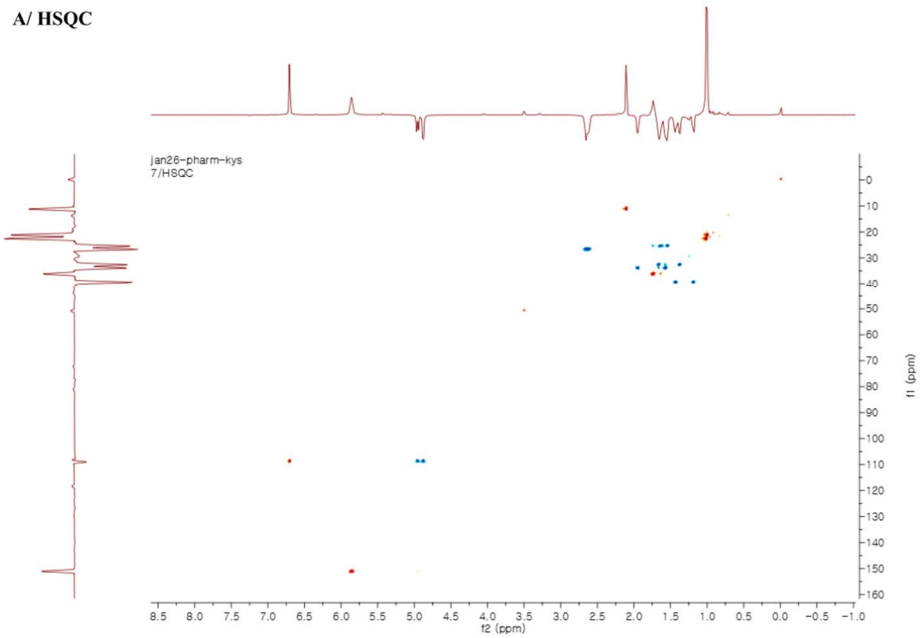

Figure 15. HSQC spectrum of H10-6 (EF) (Dissolved in $CDCl_3$, 500 MHz)

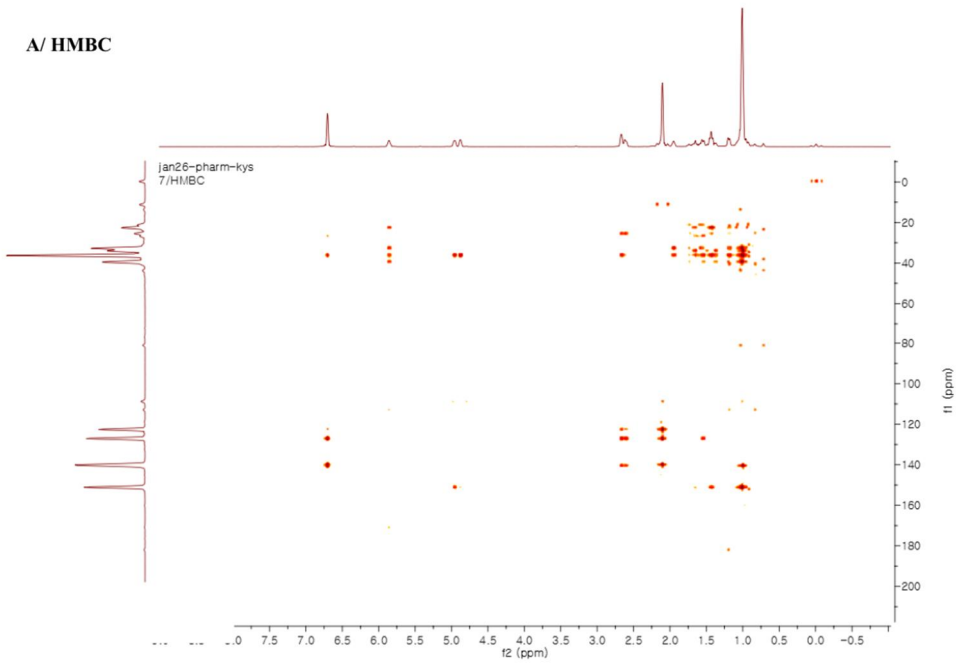

Figure 16. HMBC spectrum of H10-6 (EF) (Dissolved in $CDCl_3$, 500 MHz)

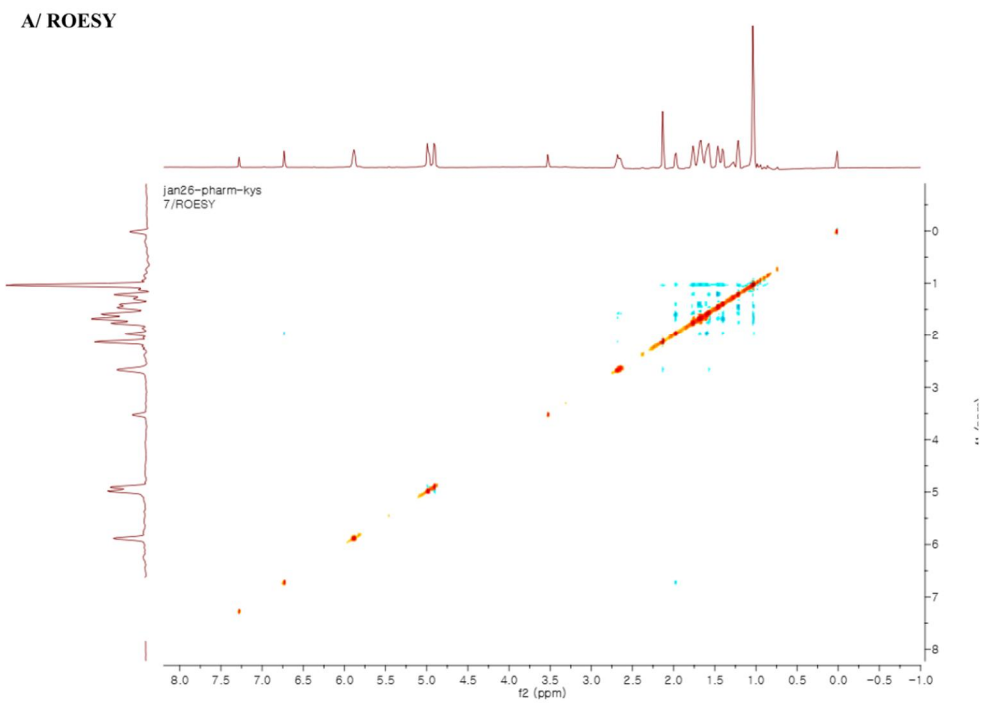

Figure 17. ROESY spectrum of H10-6 (EF) (Dissolved in $CDCl_3$, 500 MHz)

4.Effects of Ebractenoid F (EF) on pro-inflammatory mediators in LPS-stimulated RAW 264.7 cells

Besides NO and NF-κB SEAP screening (Figure 10), excessive pro-inflammatory mediators produced by macrophages, such as cytokines and chemokines, can trigger various chronic inflammatory diseases. Among them, interleukin (IL)-6, IL-1β, and MCP-1 could be regarded as potent biomarkers to evoke inflammation. In this vein of thought, the inflammatory mediators in RAW 264.7 cells were induced by LPS. The effects of EF on the inflammatory mediators were examined by real-time PCR and western blot. As a result, EF decreased the pro-inflammatory cytokines, which are interleukin (IL)-6, IL-1β, and MCP-1. Furthermore, it reduced the pro-inflammatory enzymes like inducible Nitric Oxide Synthatase (iNOS), and Cyclooxygenase-2 (COX-2) generating the inflammatory mediators (NO and PGE_2) at both mRNA and protein levels. The data indicated that EF inhibited NO, NF-κB SEAP, IL-6, IL-1 β, and MCP-1 by affecting on enzymes like iNOS and COX-2 expression at the transcriptional level (Figure 18).

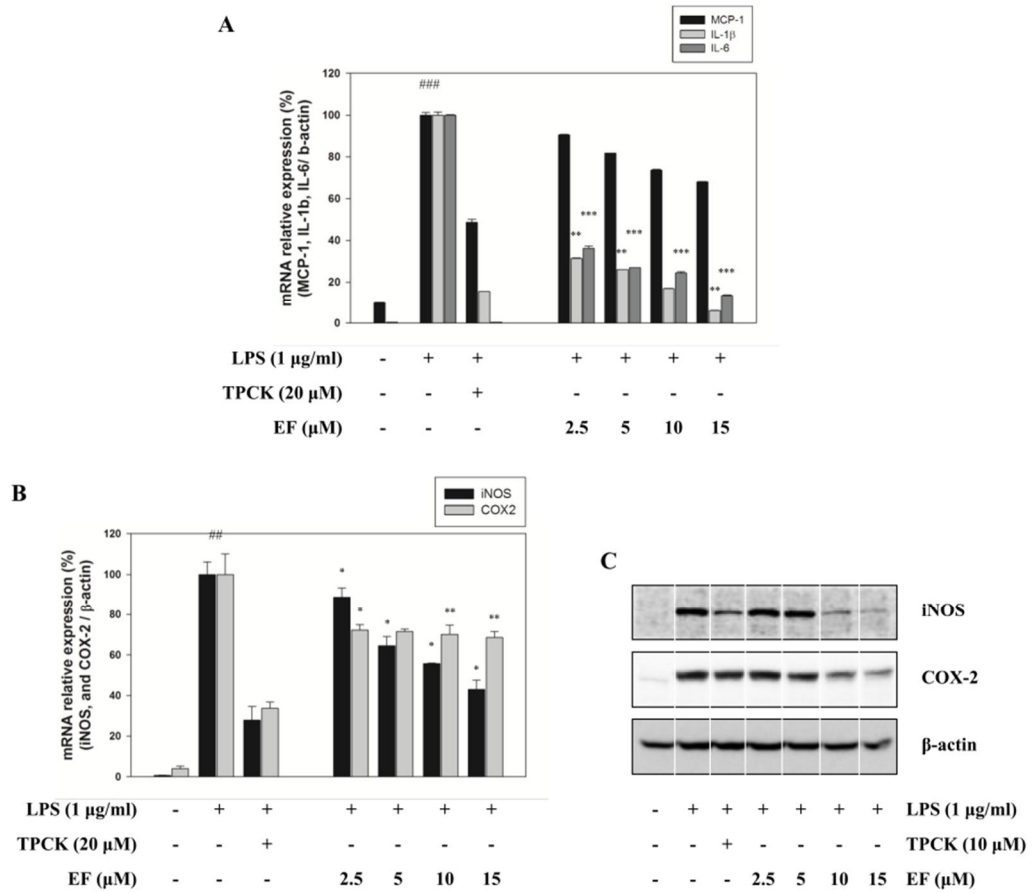

Figure 18. Ebractenoid F (EF) inhibited the downstream signaling pathways of NF-κB in LPS-stimulated RAW 264.7 cells.

Cells (1 X 10^6 cells/well) were seeded in 6-well plates and incubated for 24 h. After then, cells were pretreated with the indicated doses of the sample for 2h before LPS (1 μg/ml) stimulation.

(A) The relative level of pro-inflammatory cytokines (IL-6, IL-1β, and MCP-1) mRNA expression ($2^{-\Delta Ct}$) was determined by real-time PCR and calculated by subtracting the C_t

value for β-actin from the C_t values for IL-6, IL-1 β, and MCP-1. $\Delta C_t = C_{tIL\text{-}6 \text{ or } IL\text{-}1\ \beta \text{ or } MCP\text{-}1} - C_{t\ \beta\text{-}actin}$. (B) At the same condition like above, the relative level of pro-inflammatory enzymes (iNOS, and COX-2) mRNA expression was examined by real-time PCR. The data were obtained from three independent experiments and expressed as the means ± S.D. (C) After 18h LPS treatment, the whole lysates were subjected to Western blot analysis immunoblotting with iNOS, COX-2, and β -actin.

5. Effects of Ebractenoid F (EF) on LPS-mediated NF-κB translocational and transcriptional activity

Since NF-κB is the key regulator of inflammation, we examined whether EF affected on the NF-κB activity. After LPS stimulated RAW 264.7 cells, there were the sequential signaling pathways. To describe the effects of EF on NF-κB, when treated LPS for 15 min followed by EF (15 μM) treatment for 2 h, the extracted whole lysates and nucleus lysates were analyzed by western blot. Using the whole lysates, both inhibition of phosphorylation and degradation of iκB-α in cytosol were observed. In addition, the nuclear translocation of NF-κB dimer was attenuated by 15 μM EF treatments after 10 to 15 min LPS stimulation. Plus, NF-κB transcriptional activity by EF treatment was measured by luciferase assay. After NF-κB transfected RAW 264.7 cells were stimulated by LPS for 4-6 h, luciferase activity from the cell lysates was weakened. According to the results, we confirmed that EF could attenuate both translocational and transcriptional activity of LPS-medicated RAW 264.7 cells (Figure 19).

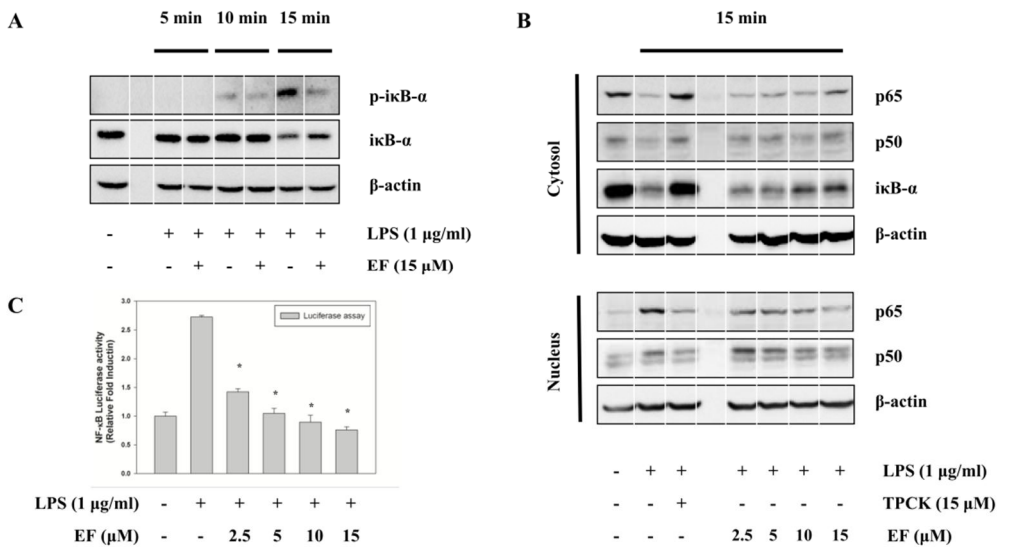

Figure 19. Ebractenoid F (EF) inhibited NF-κB in LPS-stimulated RAW 264.7 cells.

Cells (1 X 10^6 cells/well) were seeded in 6-well plates and incubated for 24 h. After then, cells were pretreated with the indicated doses of the sample for 2h before LPS (1 μg/ml) stimulation.

(A) After 0-15 min LPS treatment, the whole lysates were subjected to Western blot analysis with iκB-α, p-iκB-α, and β -actin. (B) After 0-15 min LPS treatment, cytoplasmic and nuclear extracts were extracted and analyzed by Western blot with p65, p50, iκB-α and β-actin. (C) The cells were transfected with NF-κB luciferase reporter plasmid for 4h, followed by LPS stimulation for 6h.

6. Effects of Ebractenoid F (EF) on the upstream of NF-κB and MAPKs pathway

As shown in previous results, EF regulated transcriptional and translocational activity of NF-κB. We investigated the upstream signaling pathway to regulate NF-κB. It is reported that LPS can evoke NF-κB activation via TLR4-MyD88-TIRAP pathway. EF decreased the phosphorylation of AKT and IKKα/β at the right upper factors of NF-κB. However, the uppermost factors, TLR4, MyD88, and TIRAP, were not affected by EF treatment. Hence, it may pass through the plasma membrane and specifically target on NF-κB.

As another important fact, the MAPKs pathway is one of the most extensively investigated signal transduction pathways related to inflammation process. Previous studies have reported that MAPKs pathway plays an important role during the release of pro-inflammatory cytokines and inflammatory mediators in LPS-induced RAW264.7 cells. Therefore, we examined the effects of EF on the phosphorylation levels of p38 MAPK extracellular signal-regulated kinase (ERK) and jun NH2-terminal kinase (JNK) in the presence of LPS treatment by western blot analysis. As shown in Figure 20, EF down-regulated the phosphorylation of JNK, and ERK1/2 induced by LPS stimulation within 15 min.

Through these works, we settle that EF can modulate the inflammatory transcription factor, NF-κB, by regulating the inhibitory effects of NF-κB upstream pathways (AKT, and IKK α/β) and MAPKs (JNK, and ERK1/2) signaling pathways (Figure 21).

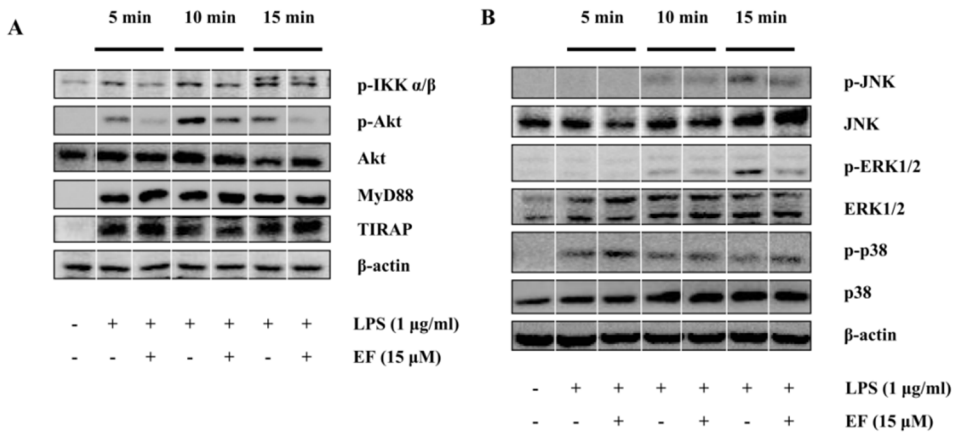

Figure 20. Ebractenoid F (EF) inhibited the upstream signaling pathways of NF-κB and MAPKs in LPS-stimulated RAW 264.7 cells.

Cells (1 X 10^6 cells/well) were seeded in 6-well plates and incubated for 24 h. After then, cells were pretreated with the indicated doses of the sample for 2h before LPS (1 μg/ml) stimulation.

Within 15min LPS treatment, the whole lysates were subjected to Western blot analysis (A) with p-Akt, Akt, p-IKK α/β, IKK α/β, MyD88, TIRAP, and β -actin. (B) with p-p38, p38, p-JNK, JNK, p-ERK1/2, ERK1/2, and β -actin.

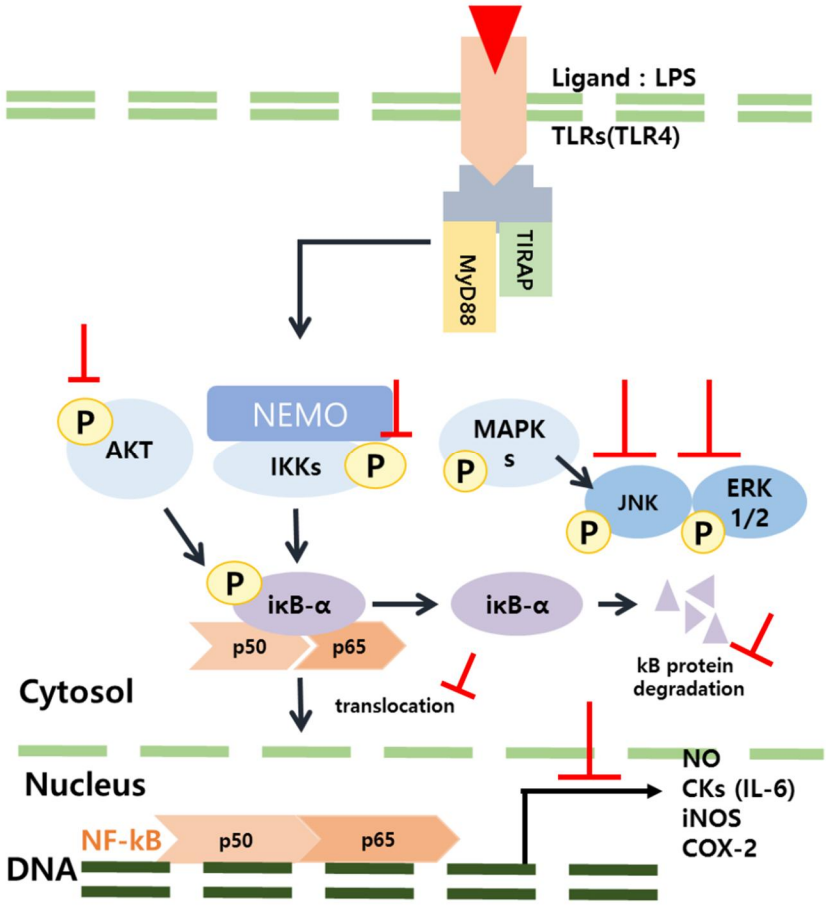

Figure x. The effects of EF on inflammatory mechanisms

IV. DISCUSSION

Understanding how the NF-κB pathway influences and is influenced by signaling pathways provides crucial insight into the regulation of inflammatory responses [29]. Though lots of treatments for inflammation-associated diseases have been launched and diagnosed, the drugs have still side-effects [4]. The studies of new agents from natural products have been conducted continuously [42]. We now know that LPS-evoked TLR4 signaling pathways are clearly related to inflammation [28], through these pathways aforementioned in figure 21.

As the efficient separation method, activity-guided fractionation and purification processes were employed to identify the anti-inflammatory compound from *Euphorbia ebracteolata* [1]. Powdered roots of the medicinal herb were extracted with ethanol and then partitioned with solvents, *n*-Hex, MC, EA, *n*-BuOH, and DW. Among them, *n*-Hex layer showed strong activity and therefore, subjected to separation and purification using various chromatographic techniques. The extract was fractionated into 1-12 fractions by HSCCC, and the fraction H10 showing potent activity was isolated using prep-LC. Isolated fraction was identified by comparing spectral data (LC-UV, NMR, and ESI-MS) with literatures [19-25, 39-41] to be a rosane-type diterpene, ebractenoid F [21, 22].

At each fractionation step, we explored whether they have toxicity *in vitro* with all the samples (extract, fractions, sub-fractions, and compounds) at first to discover

the most proficient compound by bioassay-guided fractionation against inflammation. Using the non-toxic doses, inflammatory mediators dissolved in supernatant excreted from the cells were investigated by NO assay [30, 31]. To concrete its anti-inflammatory activities, NF-κB SEAP assay was conducted as well [32]. Through all the processes, H10-6, ebractenoid F, was selected as the therapeutic agents against inflammation by narrowing the candidates.

Ebractenoid F is one of active constituents of *Euphorbia ebracteolata* [21, 22]. It has been reported that Ebractenoid F reduces nitric oxide in murine macrophages at the non-toxic doses [22]. Macrophage plays a central role in a host's defense against bacterial infection through phagocytosis, cytotoxicity, and intracellular killing [7]. Although the research has shown that ebractenoid F induced anti-inflammatory effects in macrophages, the inherent mechanism underlying the effect of EF on LPS-induced inflammation remains unknown. The results indicated that ebractenoid F decreased nitric oxide and NF-κB SEAP in supernatant into which inflammation-induced cells secreted (Fig. 10). We demonstrated that ebractenoid F can inhibit many inflammatory mediators, such as enzymes, cytokines and chemokines, which induce inflammation at both protein and mRNA levels.

Ebractenoid F suppressed iκB-α phosphorylation and degradation, staying in inactive (Fig. 11A). In addition, the results showed that ebractenoid F inhibited nuclear translocation of NF-κB and NF-κB -DNA binding activities (Fig. 11B). Furthermore, we investigated whether ebractenoid F may not only inhibit the binding of NF-κB to the DNA but it also inhibits the upstream signaling proteins.

When engaged by LPS, the LPS receptor, TLR4, transduces signals through MyD88 and TRAF6 [28]. It is possible that ebractenoid F suppresses inflammatory genes and transcription factors by blocking the TLR4 or other accessory proteins, such as MyD88 and TIRAP [14]. The induction of MyD88 and TIRAP leads to the activation of NF-κB followed by the production of pro-inflammatory cytokines [28]. PI3K, existing in a complex with TLR4 and MyD88 in murine macrophages, and its downstream target kinase, AKT, appear to be important components of LPS-induced NF-κB activation. NF-κB is also activated by NF-κB upstream signaling cascades such as IKK-α/β [29]. As a result, although ebractenoid F did not reduce the uppermost protein, TLR4, MyD88, and TIRAP, ebractenoid F had an effect on the protein levels of constitutively phosphorylated AKT and IKKs (Fig. 12A).

MAPKs are a highly conserved family of protein serine/threonine kinases and have been shown to play significant roles in inflammation induced by various stimuli [43]. MAPKs are the main kinases involved in activation of a number of downstream pathways such as ERK, JNK and p38, which are also associated with NF-κB. The result showed that ebractenoid F suppressed the phosphorylation of ERK, and JNK in a dose-dependent manner without affecting their total protein levels (Fig. 13).

In conclusion, this study provides the concrete evidence on anti-inflammatory effects of ebractenoid F. Anti-inflammatory effects of ebractenoid F are associated with its capacity to regulate p-AKT/p-IKK/NF-κB/MAPKs (p-ERK and p-JNK) activation in RAW264.7 cells. In turn, ebractenoid F can ameliorate the

inflammatory mediators at the downstream of NF-κB pathway. Based on this study, these results could offer significant information regarding the use of ebractenoid F as a candidate therapeutic agent against inflammation-mediated diseases.

REFERENCE

[1] Weller MG, A unifying review of bioassay-guided fractionation, effect-directed analysis and related techniques, Sensors, 2012, **12**:9181-9209

[2] Kellogg JJ, Todd DA, Egan JM, Raja HA, Oberlies NH, Kvalheim OM, and Cech NB, Biochemometrics for natural products research: comparison of data analysis approaches and application to identification of bioactive compounds, J Nat Prod, 2016, **79**:376-386

[3] Malviya N, and Malviya S, Bioassay guided fractionation-an emerging technique influence the isolation, identification and characterization of lead phytomolecules, International Journal of Hospital Pharmacy (IJHP), 2017, **2**:1-6

[4] Medzhitov R, Origin and physiological roles of inflammation, Nature, 2008, **454**:428-435

[5] Ingersoll MA, Platt AM, Potteaux S, and Randolph GJ, Monocyte trafficking in acute and chronic inflammation, Trends in Immunology, 2011, **32**(10):470-477

[6] Ellinghaus D, Jostins L, Spain SL, Cortes A, Bethune J, Han B, and et al, Analysis of five chronic inflammatory diseases identifies 27 new associations and highlights disease-specific patterns at shared loci, Nat Genet, 2016, **48**(5): 510-519

[7] Kotas ME, and Medzhitov R, Homeostasis, Inflammation, and Disease

Susceptibility, Cell, 2015, **160**(5):816-827

[8] Pasparakis M, and Vandenabeele P, Necroptosis and its role in inflammation, Nature, 2015, **517**:311-320

[9] Heppner FL, Ransohoff RM, and Becher B, Immune attack: the role of inflammation in Alzheimer disease, Nature Reviews, 2015, **16**:358-372

[10] Felice FGD, and Ferreira ST, Inflammation, Defective Insulin Signaling, and Mitochondrial Dysfunction as Common Molecular Denominators Connecting Type 2 Diabetes to Alzheimer Disease, Am Diabetes Assoc, 2014, **63**(7):2262-2272

[11] Cutolo M, Paolino S, and Pizzorni C, Possible contribution of chronic inflammation in the induction of cancer in rheumatic diseases, Clin Exp Rheumatol, 2014, **32**(6):839-847

[12] Takeuchi O, and Akira S, Pattern recognition receptors and inflammation, Cell, 2010, **140**:805-820

[13] Tsan MF, Toll-like receptors, inflammation and cancer, Semin Cancer Biol, 2006, **16**:32-37

[14] Yamamoto M, Sato S, Hemmi H, Sanjo H, Uematsu S, Kaisho T, and et al., Essential role for TIRAP in activation of the signaling cascade shared by TLR2 and TLR4, Nature, 2002, **420**:324-329

[15] Lee KH, Natschke SM, Qian K, Dong Y, Yang X, Zhou T, Belding E, Wu SF, Wada K, and Akiyama T, Recent Progress of Research on Herbal Products

Used in Traditional Chinese Medicine: the Herbs belonging to the divine husbandman's herbal foundation canon, J Tradit Complement Med, 2011, **2**(1): 6-26

[16] Jiang X, Liu ZG, Cao YF, Meng DL, and Hua HM, Chemotaxonomic and chemical studies on two plants from genus of *Euphorbia*: *Euphorbia fischeriana* and *Euphorbia ebracteolata*, Biochem Syst Ecol, 2014, **57**: 345-349

[17] Deng B, Mu SZ, and Hao XJ, Chemical constituents from *Euphorbia ebracteolata*, Chin J Nat Med, 2010, 8(3): 183-185

[18] Su XL, Lin RC, Wong SK, Tsui SK, and Kwan SY, Identification and characterization of the Chinese herb langdu by LC-MS/MS analysis, Phytochem Anal. 2003, **14**: 40-47

[19] Shi HM, Williams ID, Sung HH, Zhu HX, Ip NY, and Min ZD, Cytotoxic diterpenoids from the roots of *Euphorbia ebracteolata*, Planta Med, 2005, **71**:349-354

[20] Liu ZG, Li ZL, Li DH, Li N, Bai J, Zhao F, Meng DL, and Hua HM, e*nt*-Abietane-type diterpenoids from the roots of *Euphorbia ebracteolata* with their inhibitory activities on LPS-induced NO production in RAW264.7 macrophages, Bioorganic Med Chem Lett, 2016, **26**: 1-5

[21] Liu ZG, Li ZL, Bai J, Meng DL, Li N, Pei YH, Zhao F, and Hua HM. Anti-inflammatory diterpenoids from the roots of *Euphorbia ebracteolata*, J Nat Prod, 2014, **77**: 792-799

[22] Mu SZ, Jiang CR, Huang T, and Hao XJ, Two new rosane-type diterpenoids from *Euphorbia ebracteolata* Hayata, Helv Chim Acta, 2013, 96: 2299-2303

[23] Wang CJ, Jiang YQ, Liu DH, Yan XH, and MA SC. Characterization of phloroglucinol derivatives and diterpenes in *Euphorbia ebracteolata* Hayata by utilizing ultra-performance liquid chromatography/quadrupole time-of-flight mass spectrometry, J Pharm Anal, 2013, **3**(4): 292-297.

[24] Fu GM, Qin HL, Yu SS, and Yu BY, Yuexiandajisu D, a novel 18-nor-rosane-type dimeric diterpenoid from Euphorbia ebracteolata Hayata, J Asian Nat Prod Res, 2006, **8**:29-34

[25] Yin ZQ, Fan CL, Ye WC, Jiang RW, Che CT, Mak TC, Zhao SX, and Yao XS, Acetophenone derivatives and sesquiterpene from *Euphorbia ebracteolata*, Planta Med, 2005, **71**(10):979-982

[26] Pahl HL, Activators and target genes of Rel/NF-κB transcription factors, Oncogene, 1999, **18**: 6853-6866

[27] Oeckinghaus A, Hayden MS, and Ghosh S, Crosstalk in NF-κB signaling pathways, Nat Immunol, 2011, **12**(8): 695-708

[28] Lu YC, Yeh WC, and Ohashi PS, LPS/TLR4 signal transduction pathway, Cytokine, 2008, **42**(2):145-151

[29] Hoffmann A, and Baltimore D, Circuitry of nuclear factor kappaB signaling, Immunol Rev, 2006, **210**:171-186

[30] Guzic TJ, Korbut R, and Adamek-guzik T, Nitric oxide and superoxide in

inflammation and immune regulation, J Physiol and Pharmacol, 2003, **54**(4):469-487

[31] Aktan F, iNOS-mediated nitric oxide production and its regulation, Cell Mol Life Sci, 2004, **75**:639-653

[32] Erkel G, Anke T, and Sterner O, Inhibition of activation by panepoxydone, Biochem Biophys Res Commun, 1996, **226**:214-221

[33] Ito Y, Golden rules and pitfalls in selecting optimum conditions for high-speed counter-current chromatography, J Chromatogr A, 2005, **1065**:145-168

[34] A. Weisz, Y Ito, and WD Conway, High-Speed Countercurrent Chromatography, Chem Anal, 2000, 2588-2601

[35] Song K, Lee KJ, and Kim YS, Development of an efficient fractionation method for the preparative separation of sesquiterpenoids from *Tussilago farfara* by counter-current chromatography, J Chromatogr A, 2017, **1489**:107-114

[36] Liu MS, Tao L, Chau SL, Wu R, Zhang H, Yang Y, Yang D, Bian ZX, Lu A, Han Q, and Xu H, Folding fan mode counter-current chromatography offers fast blind screening for drug discovery. Case study: finding anti-enterovirus 71 agents from *Anemarrhena asphodeloides*, J Chromatogr A, 2014, **1368**: 116-124

[37] Song H, Lin J, Zhu X, and Chen Q, Developments in high-speed countercurrent chromatography and its applications in the separation of

terpenoids and saponins, J Sep Sci, 2016, **39**: 1574-1591

[38] Shinomiya K, Yoshida K, Tokura K, Tsukidate E, Yanagidaira K, and Ito Y, Countercurrent chromatographic seaparation of proteins using an eccentric coiled column with synchronous and nonsynchronous type-J planetary motions, Anal Sci, 2015, **3**:211-218

[39] Lee JW, Lee C, Jin Q, Jang H, Lee D, Lee HJ, Shin JW, Han SB, Hong JT, Kim YS, Lee MK, and Hwang BY. Diterpenoids from the roots of *Euphorbia fischeriana* with inhibitory effects on nitric oxide production, J Nat Prod, 2015, **79**: 126-131

[40] Talapatra SK, Das G, and Talapatra Bani, Stereostructures and molecular conformations of six diterpene lactones from *Gelonium multiflorum*, Phtochemistry, 1989, **28**(4): 181-1185

[41] Sun YX, and Liu JC, Chemical constituents and biological activities of *Euphorbia fischeriana* STEUD, Chem Biodivers, 2011, **8**: 1205-1214

[42] Yuan G, Wahlqvist ML, He G, Yang M, and Li D, Natural products and anti-inflammatory activity, Asia Pac J Clin Nutr, 2006, **15**:143-152

[43] Seger R, and Krebs EG, The MAPK signaling cascade, The FASEB J, 1995, **9**(9):726-735

ABSTRACT IN KOREAN（국문초록）

붉은대극（*Euphorbia ebracteolata* Hayata, Euphorbiaceae）은 중국의 남쪽 지방에 널리 분포하며, 대극과에 속하는 여러해살이 풀이다. 뿌리를 약재로 사용하며, 폐결핵, 급성 후두염 및 기관염, 건선 등 만성염증을 동반하는 질환 치료에 활용된다. 붉은대극은 acetophenones, diterpenoids, flavonoids 와 같은 화합물들을 많이 함유하며 항암, 항염증에 효능을 갖는다고 보고된다.

염증이란, 외부적 자극에 대항하고, 항상성을 유지하기 위한 방어적 기전 반응으로, 대식세포가 염증반응에 주요한 역할을 수행하며, Lipopolysaccharide (LPS) 라는 외부적 자극에 의해 Toll-like receptor 4 (TLR4)라는 세포 표면 수용체가 활성화되어 Nuclear Factor (NF)-κB (NF-κB)가 관여하는 일련의 과정을 거치게 되고, 염증 반응을 유도한다.

본 연구는 붉은대극으로부터 항염증 효능을 갖는 활성 물질을 발굴하기 위하여 Bioassay-guided 분리 기법을 활용하였다. 염증 기전에 약리적 억제효능을 갖는 물질을 선정하기 위해 nitric oxide (NO) assay 및 NF-κB Secretory Alkaline Phosphatase (SEAP) assay를 활용하였으며, 향류액체크로마토그래피 (High Speed Counter-Current Chromatography, HSCCC)와 preparative-HPLC를 이용하여 항염증 효능을 갖는 단일 화합물을 분리, 정제해 획득하였다. NF-κB SEAP을 가장 효율적으로 억제시킨 화합물들이 선별되었고, 1D 및 2D NMR로 구조를 규명하고 동정한 결과, 분리한 물질 중 신규성을 갖는 Ebractenoid F (EF) 가 최종 물질로 선정되었다. EF는 rosane-type diterpenoid 계열이며, 이는 약리적 효능에 대한 자세한 기전이 알려진 바 없어 이 화합물의 약리적 활성 기전을 규명할 가치가 있었다. 따라서, 해당 활성 화합물의 염증 매개 인자에 미치는 영향에 대해 규명하였다.

급성과 만성 염증과 연계되는 염증 관련 전사 인자인 NF-κB의 하위 기전으로 Nitric Oxide (NO)와 NF-κB SEAP을 억제시킴을 확인하였고, 그 외에 염증 사이토카이닌 (MCP-1, IL-6, IL-1β)을 억제시켰다. 염증인자를 생성해내는 효소(iNOS, COX-2) 또한 mRNA level과 protein level에서 억제시켰다. 염증 인자들을 조절하는 전사인자 NF-κB와 관련하여 세포질에서 iκBα의 인산화 및 분해, NF-κB 의 핵 내로의 전위, 핵 내에서의 전사 활성에 대한 EF의 억제 효능을 protein level에서 확인하였다. 또한, EF는 상위 인자인 AKT와 IKK-α/β 의 인산화를 억제시켜 NF-κB를 조절하였으며, 다른 염증 관련 기전에 해당하는 MAPK 기전 중, JNK, ERK의 인산화를 억제시켜 염증을 조절함을 확인할 수 있었다.
결론적으로, 붉은대극으로부터 분리한 EF가 NF-κB 신호 전달 기전을 조절함으로써 항염증에 효능을 보임을 확인하였고, 염증을 동반하는 질환 치료제 성분으로 활용 가능성을 기대할 수 있다.

주 요 어 : 붉은대극, HSCCC, NF－κB, RAW 264.7 cell

학 번 : 2016－21847